creased $O_2^{\cdot -}$ production. Infusion of AM suppressed $O_2^{\cdot -}$ production, increasing both the synthesis and bioavailability of NO—i.e., AM was able to greatly improve endothelial function. This also suggests that AM or a similarly acting analogue may represent as an ideal therapeutic agent with both antihypertensive and antioxidant properties.

Acknowledgments

This study was supported by the Grants-in-Aid for Scientific Research on Priority Areas and for the 21st Century Centers of Excellence Program (Life Science) from the Japanese Ministry of Education, Culture, Sports, Science and Technology, and by Grants-in-Aid for Research on Industrial Technology from the New Energy and Industrial Technology Development Organization (NEDO). The authors are grateful to Dr. Tsuneaki Sakada of Shionogi Co., Ltd. for kindly providing recombinant human AM. The authors also thank Dr. Seiichi Hashida for AM measurement.

References

[1] K. Kitamura, K. Kangawa, M. Kawamoto, Y. Ichiki, S. Nakamura, H. Matsuo, T. Eto, Adrenomedullin: a novel hypotensive peptide isolated from human pheochromocytoma, Biochem. Biophys. Res. Commun. 192 (1993) 553–560.

[2] Y. Ichiki, K. Kitamura, K. Kangawa, M. Kawamoto, H. Matsuo, T. Eto, Distribution and characterization of immunoreactive adrenomedullin in human tissue and plasma, FEBS Lett. 338 (1994) 6–10.

[3] S. Sugo, N. Minamino, K. Kangawa, K. Miyamoto, K. Kitamura, J. Sakata, T. Eto, H. Matsuo, Endothelial cells actively synthesize and secrete adrenomedullin, Biochem. Biophys. Res. Commun. 201 (1994) 1160–1166.

[4] C. Nuki, H. Kawasaki, K. Kitamura, M. Takenaga, K. Kangawa, T. Eto, A. Wada, Vasodilator effect of adrenomedullin and calcitonin gene-related peptide receptors in rat mesenteric vascular beds, Biochem. Biophys. Res. Commun. 196 (1993) 245–251.

[5] Y. Ishiyama, K. Kitamura, Y. Ichiki, S. Nakamura, O. Kida, K. Kangawa, T. Eto, Hemodynamic effects of a novel hypotensive peptide, human adrenomedullin, in rats, Eur. J. Pharmacol. 241 (1993) 271–273.

[6] R.W. Troughton, L.K. Lewis, T.G. Yandle, A.M. Richards, M.G. Nicholls, Hemodynamic, hormone, and urinary effects of adrenomedullin infusion in essential hypertension, Hypertension 36 (2000) 588–593.

[7] H. Hayakawa, L. Raij, The link among nitric oxide synthase activity, endothelial function, and aortic and ventricular hypertrophy in hypertension, Hypertension 29 (1997) 235–241.

[8] Y.N. Cao, K. Kitamura, K. Ito, J. Kato, S. Hashida, K. Morishita, T. Eto, Glycine-extended adrenomedullin exerts potent vasodilator effect through amidation in the rat aorta, Regul. Pept. 113 (2003) 109–114.

[9] K. Kitamura, Y. Ichiki, M. Tanaka, M. Kawamoto, J. Emura, S. Sakakibara, K. Kangawa, H. Matsuo, T. Eto, Immunoreactive adrenomedullin in human plasma, FEBS Lett. 341 (1994) 288–290.

[10] N. Hirayama, K. Kitamura, T. Imamura, J. Kato, Y. Koiwaya, T. Tsuji, K. Kangawa, T. Eto, Molecular forms of circulating adrenomedullin in patients with congestive heart failure, J. Endocrinol. 160 (1999) 297–303.

[11] J.W. Baynes, Role of oxidative stress in development of complications in diabetes, Diabetes 40 (1991) 405–412.

[12] R.W. Alexander, Theodore Cooper Memorial Lecture, Hypertension and the pathogenesis of artherosclerosis: oxidative stress and the mediation of arterial inflammatory response: a new perspective, Hypertension 25 (1995) 155–161.

[13] C. Kunsch, R.M. Medford, Oxidative stress as a regulator of gene expression in the vasculature, Circ. Res. 85 (1999) 753–766.

[14] D. Steinberg, S. Parthasarathy, T.E. Carew, J.C. Khoo, J.L. Witztum, Beyond cholesterol: modification of low-density lipoprotein that increase its artherogenicity, N. Engl. J. Med. 320 (1989) 915–920.

[15] U. Landmesser, S. Spiekermann, S. Dikalov, H. Tatge, R. Wilke, C. Kohler, D.G. Harrison, B. Hornig, H. Drexler, Vascular oxidative stress and endothelial dysfunction in patients with chronic heart failure: role of xanthine-oxidase and extracellular superoxide dismutase, Circulation 106 (2002) 3073–3078.

[16] D.J. Stuehr, Mammalian nitric oxide synthases, Biochim. Biophys. Acta 1411 (1999) 217–230.

[17] K. Schmidt, E.R. Werner, B. Mayer, H. Wachter, W.R. Kukovetz, Tetrahydrobiopterin-dependent formation of endothelium-derived relaxing factor (nitric oxide) in aortic endothelial cells, Biochem. J. 281 (1992) 297–300.

[18] T. Heitzer, C. Brockhoff, B. Mayer, A. Warnholtz, H. Mollnau, S. Henne, T. Meinertz, T. Munzel, Tetrahydrobiopterin improves endothelium-dependent vasodilation in chronic smokers: evidence for a dysfunctional nitric oxide synthase, Circ. Res. 86 (2000) e36–e41.

[19] H. Nishimatsu, Y. Hirata, T. Shindo, H. Kurihara, E. Suzuki, M. Sata, H. Satonaka, R. Takeda, D. Nagata, M. Kakoki, H. Hayakawa, K. Kangawa, H. Matsuo, T. Kitamura, R. Nagai, Endothelial responses of the aorta from adrenomedullin transgenic mice and knockout mice, Hypertens. Res. 26 (2003) S79–S84.

[20] T. Shimosawa, Y. Shibagaki, K. Ishibashi, K. Kitamura, K. Kangawa, S. Kato, K. Ando, T. Fujita, Adrenomedullin, an endogenous peptide, counteracts cardiovascular damage, Circulation 105 (2002) 106–111.

[21] T. Shimosawa, T. Ogihara, H. Matsui, T. Asano, K. Ando, T. Fujita, Deficiency of adrenomedullin induces insulin resistance by increasing oxidative stress, Hypertension 41 (2003) 1080–1085.

[22] J. Bauersachs, A. Bouloumie, D. Fraccarollo, K. Hu, R. Busse, G. Ertl, Endothelial dysfunction in chronic myocardial infarction despite increased vascular endothelial nitric oxide synthase and soluble guanylate cyclase expression, Circulation 100 (1999) 292–298.

[23] L. Li, G.D. Fink, S.W. Watts, C.A. Northcott, J.J. Galligan, P.J. Pagano, A.F. Chen, Endothelin-1 increases vascular superoxide via endothelin(A)-NADPH oxidase pathway in low-renin hypertension, Circulation 107 (2003) 1053–1058.

[24] J. Yamaga, S. Hashida, K. Kitamura, M. Tokashiki, T. Aoki, H. Inatsu, N. Ishikawa, K. Kangawa, K. Morishita, T. Eto, Direct measurement of glycine-extended adrenomedullin in plasma and tissue using an ultrasensitive immune complex transfer enzyme immunoassay in rats, Hypertension Res. 26 (2003) S45–S53.

[25] A. Swei, F. Lacy, F.A. Delano, G.W. Schmid-Schonbein, Oxidative stress in the Dahl hypertensive rat, Hypertension 30 (1997) 1628–1633.

[26] S. Meng, L.J. Roberts II, G.W. Cason, T.S. Curry, R.D. Manning Jr., Superoxide dismutase and oxidative stress in Dahl salt-sensitive and -resistant rats, Am. J. Physiol. 283 (2002) 732–738.

[27] J. Vasquez-Vivar, B. Kalyanaraman, P. Martasek, N. Hogg, B.C. Masters, H. Karoui, P. Tordo, K.A. Prichard Jr., Superoxide

generation by endothelial nitric oxide synthase: the influence of cofactors, Proc. Natl. Acad. Sci. USA 95 (1998) 9220–9225.
[28] R.M. Wever, T. van Dam, H.J. van Rijn, F. de Groot, T.J. Rabelink, Tetrahydrobiopterin regulates superoxide and nitric oxide generation by recombinant endothelial nitric oxide synthase, Biochem. Biophys. Res. Commun. 237 (1997) 340–344.
[29] Y. Xia, A.L. Tsai, V. Berka, J.L. Zweier, Superoxide generation from endothelial nitric oxide synthase. A Ca^{+}/calmodulin-dependent and tetrahydrobiopterin regulatory process, J. Biol. Chem. 273 (1998) 25804–25808.
[30] F. Cosentino, Z.S. Katusic, Tetrahydrobiopterin and dysfunction of endothelial nitric oxide synthase in coronary arteries, Circulation 91 (1995) 139–144.
[31] F. Cosentino, S. Patton, L.V. d'Uscio, E.R. Werner, G. Werner-Felmayer, P. Moreau, T. Malinski, T.F. Luscher, Tetrahydrobiopterin alters superoxide and nitric oxide release in prehypertention rats, J. Clin. Invest. 101 (1998) 1530–1537.
[32] T.J. Guzik, S. Mussa, D. Gastaldi, J. Sadowski, C. Ratnatunga, R. Pillai, K.M. Channon, Mechanisms of increased vascular superoxide production in human diabetes mellitus: role of NAD(P)H oxidase and endothelial nitric oxide synthase, Circulation 105 (2002) 1656–1662.
[33] S. Cai, N.J. Alp, D. McDonald, I. Smith, J. Kay, L. Canevari, S. Heales, K.M. Channon, GTP cyclohydrolase I gene transfer augments intracellular tetrahydrobiopterin in human endothelial cells: effects on nitric oxide synthase activity, protein levels and dimerisation, Cardiovasc. Res. 55 (2002) 838–849.
[34] J.S. Zheng, X.Q. Yang, K.J. Lookingland, G.D. Fink, C. Hesslinger, G. Kapatos, I. Kovesdi, A.F. Chen, Gene transfer of human guanosine 5′-triphosphate cyclohydrolase I restores vascular tetrahydrobiopterin level and endothelial function in low renin hypertension, Circulation 108 (2003) 1238–1245.
[35] Z. Huang, J. Li, Z. Jiang, Y. Qi, C. Tang, J. Du, Effects of adrenomedullin, C-type natriuretic peptide, and parathyroid hormone-related peptide on calcification in cultured rat vascular smooth muscle cells, J. Cardiovasc. Pharmacol. 42 (2003) 89–97.
[36] Y. Shimekake, K. Nagata, S. Ohta, Y. Kambayashi, H. Teraoka, K. Kitamura, T. Eto, K. Kangawa, H. Matsuo, Adrenomedullin stimulates two signal transduction pathways, cAMP accumulation and Ca^{2+} mobilization, in bovine aortic endothelial cells, J. Biol. Chem. 270 (1995) 4412–4417.
[37] M. Yamasaki, J. Kawai, T. Nakaoka, T. Ogita, A. Tojo, T. Fujita, Adrenomedullin overexpression to inhibit cuff-induced arterial intimal formation, Hypertension 41 (2003) 302–307.
[38] T. Tokudome, T. Horio, F. Yoshihara, S. Suga, Y. Kawano, M. Kohno, K. Kangawa, Adrenomedullin inhibits doxorubicin-induced cultured rat cardiac myocyte apoptosis via a cAMP-dependent mechanism, Endocrinology 143 (2002) 3515–3521.
[39] X. Zhang, T.H. Hintze, cAMP signal transduction cascade, a novel pathway for the regulation of endothelial nitric oxide production in coronary blood vessels, Arterioscler. Thromb. Vasc. Biol. 21 (2001) 797–803.
[40] R. Yoshimoto, M. Mitsui-Saito, H. Ozaki, H. Karaki, Effects of adrenomedullin and calcitonin gene-related peptide on contractions of the rat aorta and porcine coronary artery, Br. J. Pharmacol. 123 (1998) 1645–1654.
[41] K. Hirayama, M. Shimoji, L. Swick, A. Meyer, G. Kapatos, Characterization of GTP cyclohydrolase I gene expression in the human neuroblastoma SKN-BE (2)M17: enhanced transcription in response to cAMP is conferred by the proximal promoter, J. Neurochem. 80 (2002) 938–939.
[42] U. Hink, H. Li, H. Mollnau, M. Oelze, E. Matheis, M. Hartmann, M. Skatchkov, F. Thaiss, R.A. Stahl, A. Warnholtz, T. Meinertz, K. Griendling, D.G. Harrison, U. Forstermann, T. Munzel, Mechanisms underlying endothelial dysfunction in diabetes mellitus, Circ. Res. 88 (2001) e14–e22.
[43] H. Mollnau, M. Wendt, K. Szocs, B. Lassegue, E. Schulz, M. Oelze, H. Li, M. Bodenschatz, M. August, A.L. Kleschyov, N. Tsilimingas, U. Walter, U. Forstermann, T. Meinertz, K. Griendling, T. Munzel, Effects of angiotensin II infusion on the expression and function of NAD(P)H oxidase and components of nitric oxide/cGMP signaling, Circ. Res. 90 (2002) e58–e65.
[44] G.R. Drummond, H. Cai, M.E. Davis, S. Ramasamy, D.G. Harrison, Transcriptional and posttranscriptional regulation of endothelial nitric oxide synthase expression by hydrogen peroxide, Circ. Res. 86 (2000) 347–354.
[45] S. Milstien, Z. Katusic, Oxidation of tetrahydrobiopterin by peroxynitrite: implications for vascular endothelial function, Biochem. Biophys. Res. Commun. 263 (1999) 681–684.
[46] K. Kato, H. Yin, J. Agata, H. Yoshida, L. Chao, J. Chao, Adrenomedullin gene delivery attenuates myocardial infarction and apoptosis after ischemia and reperfusion, Am. J. Physiol. Heart Circ. Physiol. 285 (2003) 1506–1514.
[47] M.S. Zhou, A.G. Adam, E.A. Jaimes, L. Raij, In salt-sensitive hypertension, increased superoxide production is linked to functional upregulation of angiotensin II, Hypertension 42 (2003) 945–951.
[48] J. Zanzinger, J. Czachurski, Chronic oxidative stress in the RVLM modulates sympathetic control of circulation in pigs, Pflugers Arch. 439 (2000) 489–494.
[49] T. Shokoji, A. Nishiyama, Y. Fujisawa, H. Hitomi, H. Kiyomoto, N. Takahashi, S. Kimura, M. Kohno, Y. Abe, Renal sympathetic nerve responses to tempol in spontaneous hypertensive rats, Hypertension 41 (2003) 266–273.

ELSEVIER

Cardiovascular Research 65 (2005) 921–929

Cardiovascular Research

www.elsevier.com/locate/cardiores

Antifibrotic effect of adrenomedullin on coronary adventitia in angiotensin II-induced hypertensive rats

Toshihiro Tsuruda[a,b,*], Johji Kato[a], Kinta Hatakeyama[c], Hiroyuki Masuyama[a], Yuan-Ning Cao[a], Takuroh Imamura[a], Kazuo Kitamura[a], Yujiro Asada[c], Tanenao Eto[a]

[a]*First Department of Internal Medicine, Miyazaki Medical College, University of Miyazaki, 5200 Kihara Kiyotake, Miyazaki 889-1692, Japan*
[b]*Department of Nutrition Management, Faculty of Health and Nutrition, Minami-Kyushu University, Japan*
[c]*First Department of Pathology, Miyazaki Medical College, University of Miyazaki, Japan*

Received 2 September 2004; received in revised form 29 October 2004; accepted 3 November 2004
Available online 24 November 2004
Time for primary review 26 days

Abstract

Objective: The extracellular matrix (ECM) determines the structural integrity of the heart and vasculature, participating in cardiovascular remodeling. We previously reported that adrenomedullin (AM) inhibited cellular proliferation and protein synthesis of cardiac fibroblasts; however, the precise mechanisms of AM actions as an antifibrotic factor remain unknown. The purpose of this study was to examine the biological actions of AM against the profibrotic factor angiotensin II (Ang II) in coronary adventitia.

Methods and results: Rats with hypertension induced by Ang II infusion were administered 0.06 μg/kg/min recombinant human AM subcutaneously for 14 days. The AM infusion significantly ($p<0.05$) reduced the Ang II-induced increase of coronary adventitial fibroblasts expressing Ki-67 and α-smooth muscle actin (α-SMA) in the left ventricle, by 65%, and 62%, respectively, without affecting systolic blood pressure, left ventricle/body weight, or cross-sectional area of myocardial fibers. Collagen deposition of coronary arteries was reduced by the AM infusion (−24%, $p<0.01$), and these effects of AM were accompanied by significant reductions in gene expression of type I collagen (−49%, $p<0.05$) and transforming growth factor-β1 (TGF-β1) (−55%, $p<0.01$). In cultured cardiac fibroblasts, 10^{-7} mol/L AM exerted an inhibitory effect on TGF-β1-induced α-SMA expression ($p<0.01$) that was mimicked by 8-bromo-cAMP and attenuated by the protein kinase A inhibitor H-89.

Conclusion: AM decreased Ang II-induced collagen deposition surrounding the coronary arteries, inhibiting myofibroblast differentiation and expressions of ECM-related genes in rats. The present findings further support the biological action of AM as an antifibrotic factor in vascular remodeling.

Keywords: Extracellular matrix; Fibrosis; Hypertension; Peptide hormone; Remodeling

1. Introduction

Cardiac fibrosis is an important clinical disorder leading to deleterious consequences for myocardial function such as systolic and diastolic heart failure [1]. Particularly, thickening of the adventitia surrounding intramyocardial coronary arteries, where extracellular matrix (ECM) first accumulates in response to systemic hypertension, has been thought to reduce oxygen and nutrient supply to the *myocardium*, resulting in deterioration of ventricular function [2]. Emerging concepts of vascular remodeling underline the importance of the ECM scaffold in the vessel wall. The activated adventitial fibroblasts, known as myofibroblasts characterized by α-smooth muscle actin (α-SMA) expression, play important roles in the pathological vascular remodeling [3,4]. Therefore, both understanding of the regulation of fibroblast activation and the

* Corresponding author. First Department of Internal Medicine, Miyazaki Medical College, University of Miyazaki, 5200 Kihara Kiyotake, Miyazaki 889-1692, Japan. Tel.: +81 985 85 0872; fax: +81 985 85 6596.
E-mail address: ttsuruda@med.miyazaki-u.ac.jp (T. Tsuruda).

0008-6363/$ - see front matter © 2004 European Society of Cardiology. Published by Elsevier B.V. All rights reserved.
doi:10.1016/j.cardiores.2004.11.004

development of effective pharmacological intervention to manipulate fibroblast function are necessary to attenuate adverse remodeling.

A body of evidence suggests that the renin–angiotensin–aldosterone system is an important factor in progression of myocardial and vascular fibrosis accompanied by upregulation of transforming growth factor-β1 (TGF-β1) [5–7]. TGF-β1 induces a phenotypic change of fibroblasts to myofibroblasts in hypertensive heart disease, coronary restenosis following angioplasty, and in the healing process after myocardial infarction [8,9]. Blockage of TGF-β1 signaling was indeed reported to prevent fibroblast proliferation and diastolic cardiac dysfunction [10].

Adrenomedullin (AM), initially isolated from human pheochromocytoma [11], has been reported to have multiple functions in the cardiovascular system [12]. We and others have previously reported that AM inhibited proliferation and collagen synthesis induced by angiotensin II (Ang II) in cardiac fibroblasts of neonatal rats in vitro [13,14], suggesting a possible role of AM in attenuating cardiovascular remodeling. However, the precise mechanism by which AM acts as an antifibrotic factor in vivo remains to be elucidated.

Based upon previous studies, we hypothesized that activation of adventitial fibroblasts would result in coronary matrix remodeling in rats infused with Ang II and that pharmacological intervention with AM would lead to attenuation of perivascular fibrosis by modulating fibroblast function. Our aim in this study was to examine the biological action of AM against the profibrotic factor Ang II in coronary adventitia of rats.

2. Methods

2.1. Animals experiments

Eight-week-old male Wistar rats (Charles River Japan) weighing 200 to 250 g were housed in a temperature- and light-controlled room (25±1 °C; 12/12-h light/dark cycle) with normal rat chow and water given ad libitum. The rats were divided into three groups: control group (n=5) and two Ang II-infused groups with (n=11) or without (n=15) AM treatment. They were implanted with miniosmotic pumps (Alzet model 2002) under pentobarbital sodium anesthesia, that released either saline or 250 ng/kg/min Ang II for 14 days. In the Ang II-infused groups, another pump was implanted to infuse saline or 0.06 μg/kg/min of recombinant human AM (Shionogi & Co., Japan). The dose of AM used in this study was determined by referring to our previous observation, in which cardiac remodeling after myocardial infarction was significantly inhibited without affecting systemic blood pressure [15]. Blood pressure was measured while awake at least 9 times by tail-cuff plethysmography (Softron, BP-98A), and the mean value was recorded. At day 14, the rats were killed by decapitation and trunk blood was collected for measuring AM concentration. Plasma levels of human and rat AM were determined with commercially available immunoradiometric assay kits (Shionogi & Co., Japan). After removing atria and right ventricle of the heart, left ventricle was frozen in liquid nitrogen or fixed in 10% formalin and was embedded in paraffin wax.

The present study was performed in accordance with the Animal Welfare Act and with approval of the University of Miyazaki Institutional Animal Care and Use Committee (2003-023). This investigation confirmed with the Guide for the Care and Use of Laboratory Animals published by the US National Institutes of Health (NIH Publication No. 85-23, revised 1996).

2.2. Histology and immunohistochemistry

Ventricular tissues, fixed in 10% formalin and embedded in paraffin, were sectioned at 2 μm thickness. After deparaffinization with xylene and graded alcohol, slides were immersed in 3% H_2O_2 in methanol to block endogenous peroxidase activities, thereafter incubated with 5% skim milk to reduce the nonspecific background. The section slides were then stained with either anti-monoclonal α-SMA antibody (Clone 1A4, DAKO) at a dilution of 1:200, or antipolyclonal TGF-β1 antibody (sc-146, Santa Cruze) at 1:100 at 4 °C. After the overnight reaction with antibodies, the slide sections were incubated with EnVision+ (DAKO) for 30 min, visualized with 0.05% 3, 3′ -diaminobenzidine containing hydrogen peroxide, and counterstained with hematoxylin. For detection of Ki-67 antigen, a nuclear protein expressed in proliferating cells, tissue sections were autoclaved at 121 °C for 10 min in 10 mmol/L citrate buffer (pH 6.0) prior to incubation with primary antibody (Clone MIB-5, DAKO) at a dilution of 1:25. For the detection of collagen, slides were incubated with 0.1% picrosirius red (Direct Red 80, Sigma) dissolved in saturated picric acid for 10 min as described before [15]. The specificity of the antibody for TGF-β1 was confirmed by substitution of nonimmune rabbit serum and the absorption test as described before [16].

2.3. Morphology and cell counting

Morphological evaluation and cell counting of coronary arteries sectioned at the middle portion in the left ventricle were performed by a single observer in a blind manner. Each section immunostained with the antibody against either Ki-67 or α-SMA was scanned at a magnification of ×200, and the number of positive cells surrounding the coronary artery was determined. At least five images of fibrosis areas surrounding the blood vessel were randomly selected from each slide, and examined using an image

analysis system (Axio Vison 2.05 Carl ZEISS, Munchen, Germany) to calculate ratios of the perivascular fibrosis area to the total vascular area. To evaluate the interstitial fibrosis, collagen volume fraction in the interstitial space between myocardial fibers was determined by calculating the ratio of collagen area to the selected myocardial tissue area as previously described [15]. To measure the *cardiocyte* size, cross-sectional area of *myocardial fiber* was measured at the level of nuclei in at least 10 *cardiocytes* as described before [16]. Longitudinal- or oblique-sectioned *cardiocytes* were excluded for the analysis.

2.4. Gene expression

Gene expressions for TGF-β1 and type 1 collagen in total RNA isolated from left ventricle were measured by using real time-quantitative PCR (Prism 7700 Sequence Detector, Applied Biosystems) as previously described [17]. cDNA reverse transcribed from total RNA was amplified with the following oligonucleotide probes labeled with 6-carboxy-fluorescencein as reporter fluorescence and 6-carboxy tetramethyl-rhodamine as quencher fluorescence: TGF-β1 [18], TACGCCTGAGTGGCTGTCTTTTGA (nucleotide 985–1008); type 1 collagen [19], ACTGGAGACAGAGGA-CCGCGTGGAC (nucleotide 103–127); 18*S* ribosomal RNA [20], TGCCGACGGGCGCTGACC (nucleotide 176–193) and with the following pairs of oligonucleotides: TGF-β1 [18], TTCCTGGCGTTACCTTGGT (nucleotide 943–961, forward primer) and GCCACTGCCGGACAACT (nucleotide 1018–1034, reverse primer); type 1 collagen [19], TGCTGCTTGCAGTAACGTCG (nucleotide 32–51, forward primer) and TCAACACCATCTCTGCCTCG (nucleotide 148–167, reverse primer); 18*S* rRNA [20], CTTTGGTCGCTCGCTCCTC (nucleotide 118–136, forward primer) and CTGACCGGGTTGGTTTTGAT (nucleotide 229–248, reverse primer). The PCR products electrophoresed were observed at the expected molecular sizes, and the gene expression levels were normalized relative to that of 18*S* rRNA.

2.5. Cell culture

Cultured cardiac fibroblasts of neonatal rats were prepared as previously described [13]. After achieving confluence in the DMEM/F12 medium with 10% FBS, the cells were incubated with serum-free medium containing 5 μg/mL insulin, 5 μg/mL transferrin, and 5 ng/mL sodium selenite for 24 h. The medium was then exchanged for fresh serum-free medium described above and incubated with or without synthetic rat AM (Peptide Institute, Osaka, Japan), recombinant human TGF-β1 or 8-bromo-cAMP (Sigma, MO, USA). In another series of experiment, H-89 (Seikagaku, Tokyo, Japan), a specific protein kinase A inhibitor, was added to culture medium at least 30 min before the incubation with AM or TGF-β1.

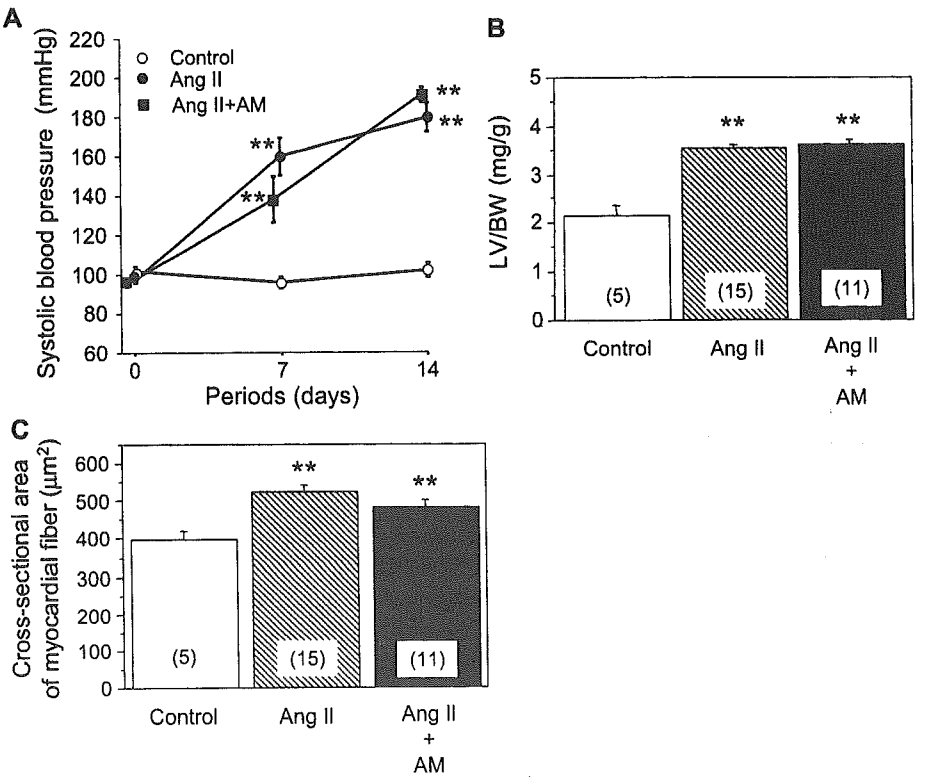

Fig. 1. Effects of Ang II and co-administration of AM on systolic blood pressure (A), left ventricular weight/body weight (LV/BW) (B), and *cross-sectional area of myocardial fiber* (C). Values are shown as means±S.E.M. Parentheses indicate the numbers of rats examined. $^{**}p<0.01$, compared to controls.

2.6. Western blot

Denatured protein extract (5 μg) from the cultured cardiac fibroblasts was subjected to sodium dodecyl sulfate–polyacrylamide gel as previously described [21]. The separated proteins were electrically transferred onto polyvinylidene difluoride (PVDF) membranes (BIO-RAD). Equal protein loading was verified by staining the gels with Coomassie brilliant blue. After blocking the non-specific background with 5% skim milk, PVDF membranes were incubated with the anti-α-SMA monoclonal antibody at a dilution of 1:1000, followed by incubation with horseradish peroxidase-coupled second antibody. Immunoreactive bands were visualized by the ECL Plus detection kit (Amersham), and intensities of the bands were analyzed densitometrically (Chemi Doc™ Documentation System, BIO-RAD).

2.7. Statistical analysis

All data are expressed as means±S.E.M. Comparisons between groups were assessed with one-way ANOVA followed by the Fisher's test. A statistical significance was accepted at $p<0.05$.

3. Results

3.1. Systolic blood pressure, left ventricle/body weight, and cardiocyte size

Fig. 1A illustrates the effects of Ang II and AM on systolic blood pressure. Continuous, subcutaneous Ang II infusion significantly ($p<0.01$) increased systolic blood pressure at days 7 and 14, and the co-administration of AM

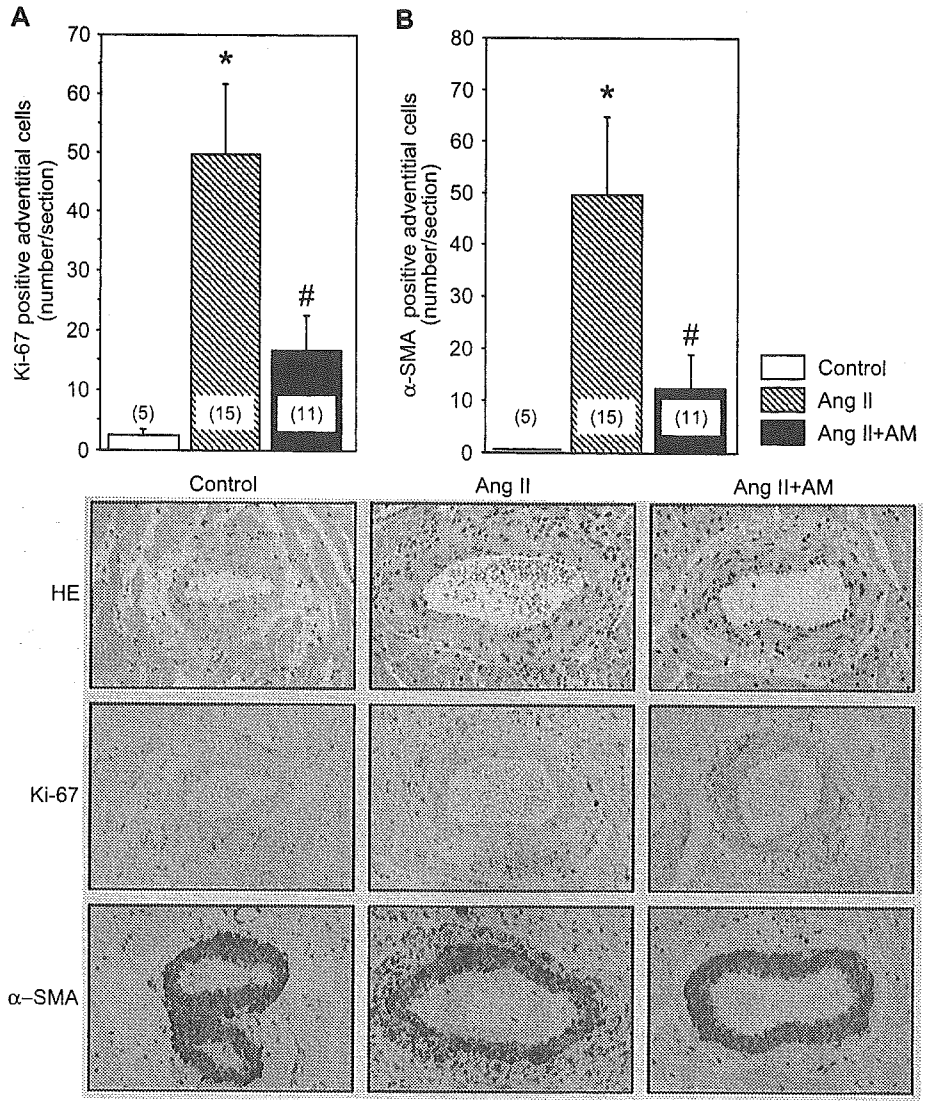

Fig. 2. Effects of Ang II and AM on the number of adventitial fibroblasts expressing Ki-67 antigen (A) and of those positive for α-SMA (B). The bottom panels show the representative histological sections stained with hematoxylin eosin (HE), anti-Ki-67, and α-SMA antibodies. Values are shown as means±S.E.M. Parentheses indicate the number of rats examined. *$p<0.05$, compared to controls; #$p<0.05$, compared to Ang II group.

with Ang II did not affect systolic blood pressure significantly. In addition, Ang II significantly ($p<0.01$) increased the left ventricle/body weight (LW/BW) and *cross-sectional area of myocardial fiber*, compared to control at day 14, without a significant difference in LV/BW or *cardiocyte* size between the Ang II and Ang II+AM groups (Fig. 1B and C).

3.2. Fibroblast proliferation and myofibroblast differentiation

Fig. 2A and B illustrate the effects of Ang II and AM on staining for Ki-67 antigen and α-SMA in the perivascular area of coronary arteries. Ang II significantly ($p<0.01$) increased the number of fibroblasts expressing Ki-67 antigen, a marker for proliferating fibroblasts, and this increase was significantly ($p<0.05$) inhibited by the co-administration of AM at day 14 (Fig. 2A). Similarly, the Ang II-induced increase in number of the fibroblasts expressing α-SMA, a marker for myofibroblast differentiation, was significantly ($p<0.05$) reduced by AM (Fig. 2B).

3.3. Type 1 collagen gene expression and adventitial area

Fig. 3A illustrates the effects of Ang II and AM on type 1 collagen mRNA expression. The Ang II infusion significantly ($p<0.05$) increased type 1 collagen expression in the left ventricle, and the co-administration of AM significantly ($p<0.05$) attenuated its expression by 49% at day 14. The effects of Ang II and AM on the adventitial area surrounding the coronary arteries are shown in Fig. 3B as composite data and in Fig. 3C as representative pictures. Ang II significantly ($p<0.01$) increased perivascular fibrosis at day 14, and the co-administration of AM significantly ($p<0.01$) decreased it. Similarly, the Ang II infusion significantly increased interstitial fibrosis of the left ventricular myocardium (+130%, $p<0.01$), while AM inhibited this Ang II effect (−54%, $p<0.01$).

3.4. TGF-β1 expression

As shown in Fig. 4A, Ang II significantly ($p<0.01$) increased TGF-β1 gene expression in the left ventricle, while the co-administration of AM significantly ($p<0.01$) attenuated its expression by 55%. Fig. 4B illustrates the distribution of TGF-β1 immunoreactivity in the coronary arteries. TGF-β1 immunoreactivity was intensely stained in the adventitial fibroblasts, as well as in vascular smooth muscle cells and *myocardial fibers* of the Ang II-treated rats, while those cells were faintly stained in the control and AM-treated rats.

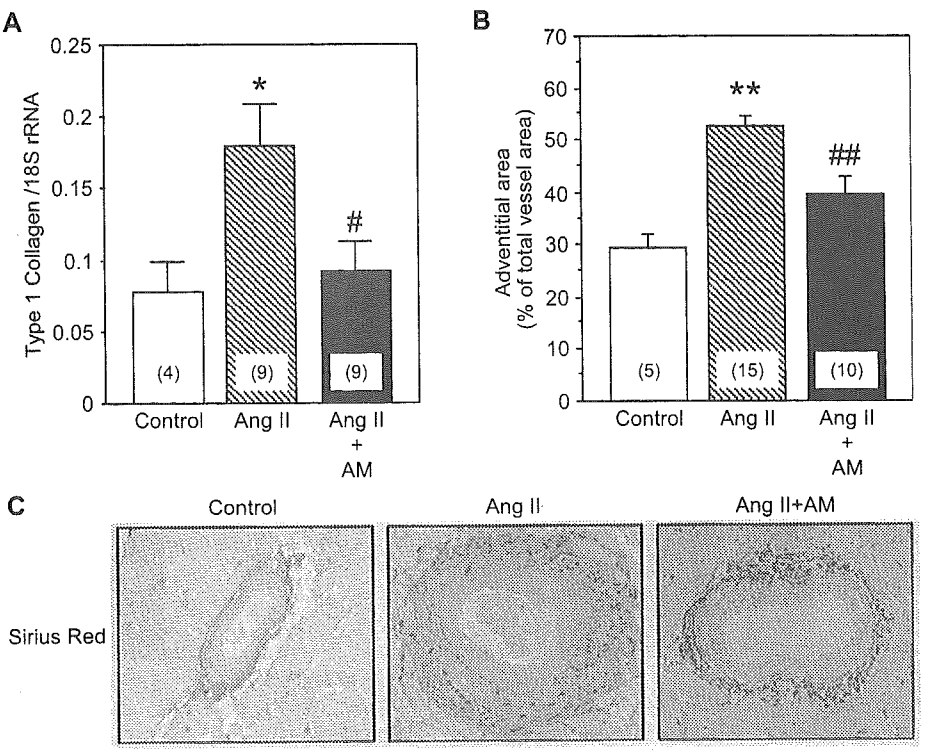

Fig. 3. Effects of Ang II and AM on gene expression of type 1 collagen (A) and on adventitial area determined by sirius red staining (B). The bottom panels (C) show the representative pictures for sirius red staining. Values are shown as means±S.E.M. Parentheses indicate the numbers of rats examined. *$p<0.05$, **$p<0.01$, compared to controls; $^{\#}p<0.05$, $^{\#\#}p<0.01$, compared to Ang II.

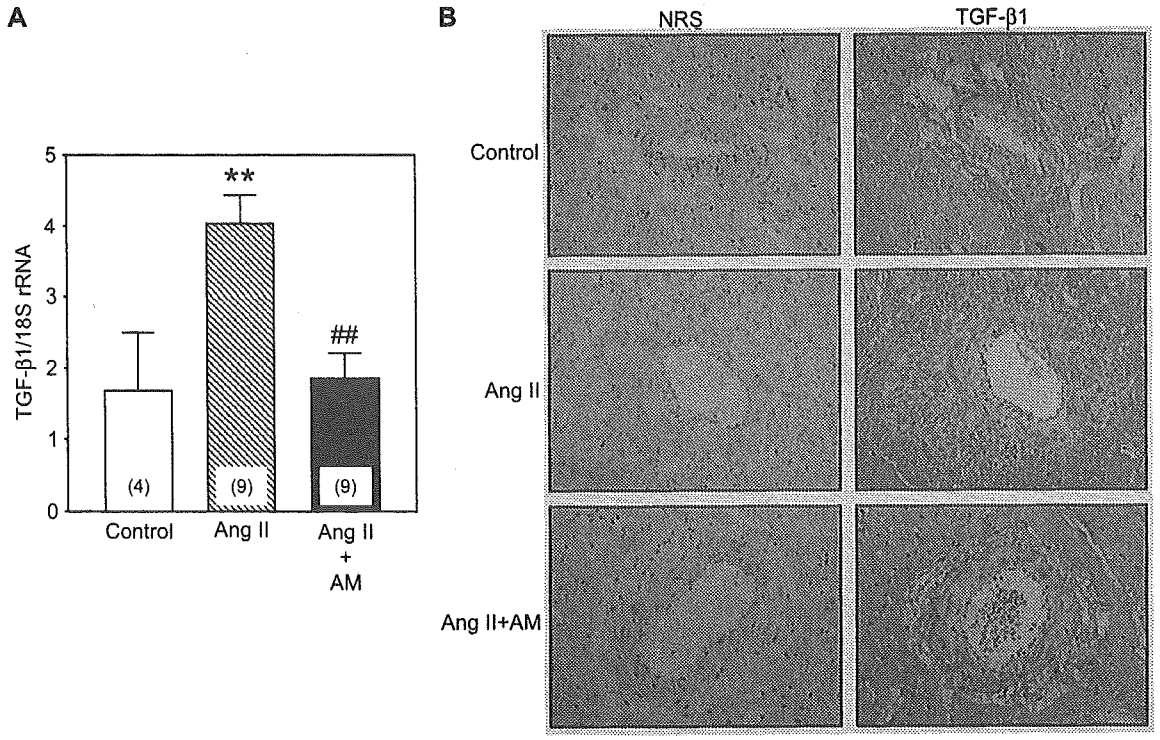

Fig. 4. Effects of Ang II and AM on the gene expression of TGF-β1 in LV (A) and representative pictures for the distribution of TGF-β1 immunoreactivity (B). Values are shown as means±S.E.M. Parentheses indicate the numbers of rats examined and NRS denotes nonimmune rabbit serum. $^{**}p<0.01$, compared to controls; $^{\#\#}p<0.01$, compared to Ang II.

3.5. Plasma levels of rat and human AM

The Ang II infusion had no significant effect on the plasma levels of endogenous rat AM at day 14 (control, 4.7±0.5; Ang II, 5.0±0.3 fmol/mL). Human AM immunoreactivity was detectable only in the plasma of recombinant AM-treated rats at 0.7±0.4 fmol/mL at day 14.

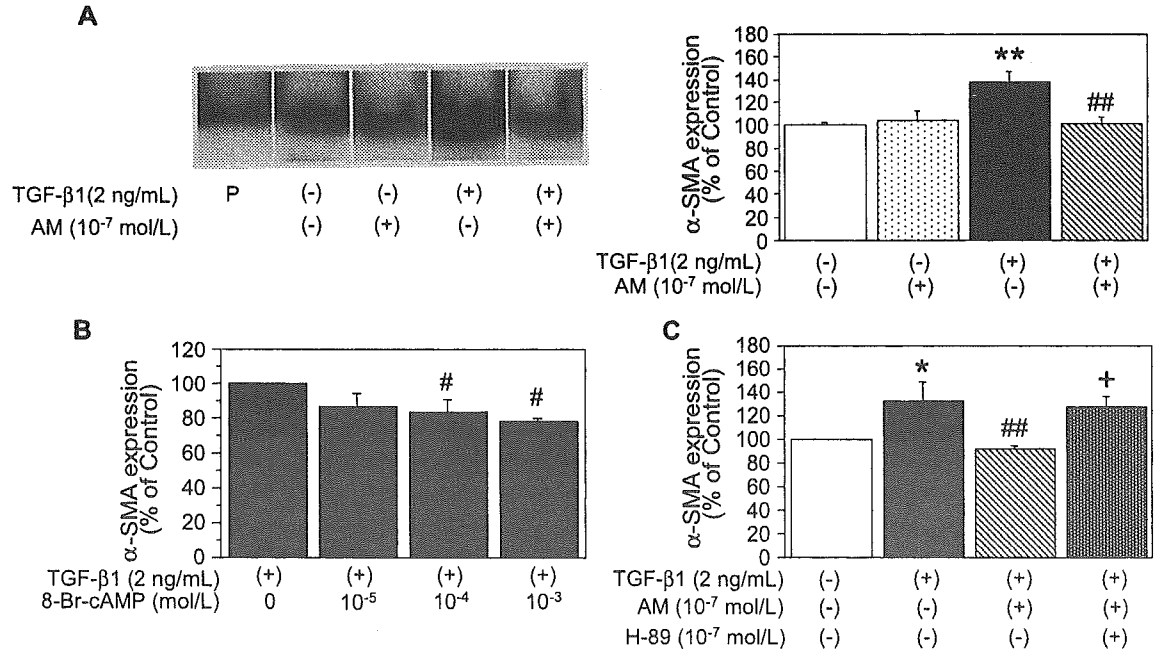

Fig. 5. Effects of AM (A), 8-bromo-cAMP (8-Br-cAMP; B), and H-89, a protein kinase A inhibitor (C) on the α-SMA expression stimulated by TGF-β1 in cultured cardiac fibroblasts. Values are shown as the means±S.E.M. of 5 to 7 (A), 3 (B), and 5 (C) samples examined. $^{*}p<0.05$, $^{**}p<0.01$, compared to controls; $^{\#}p<0.05$, $^{\#\#}p<0.01$ compared to 2 ng/mL TGF-β1; $^{+}p<0.05$, compared to TGF-β1 plus AM. P: human aorta.

3.6. α-SMA expression in vitro

To further clarify the direct action of AM on myofibroblast phenotypic change, cultured cardiac fibroblasts were treated with TGF-β1 and/or AM to look at the expression level of α-SMA. Fig. 5A illustrates a representative Western blot and the composite data. Two ng/mL TGF-β1 significantly ($p<0.01$) increased the α-SMA expression by 38% in these cells. Treatment with 10^{-7} mol/L AM significantly ($p<0.01$) inhibited the TGF-β1-induced α-SMA expression by 27%. Similarly, 8-bromo-cAMP, an analogue of cyclic AMP (cAMP), inhibited the α-SMA expression induced by TGF-β1 (Fig. 5B); while pretreatment with 10^{-7} mol/L H-89, a specific protein kinase A inhibitor, significantly ($p<0.05$) attenuated the action of AM (Fig. 5C).

4. Discussion

In this study, we report that AM attenuates the Ang II-induced perivascular fibrosis of coronary arteries, suppressing myofibroblast differentiation and expressions of TGF-β1 and type 1 collagen, without affecting blood pressure, left ventricular weight, and cross-sectional area of myocardial fiber. Ventricular remodeling characterized by *myocardial* hypertrophy and fibrosis results in serious consequences for cardiac function. Remodeling of the myocardium involves alteration of the function of fibroblasts, the major cells making up two-thirds of the total cell number in the heart [22]. Fibroblasts change their phenotype to myofibroblasts capable of producing ECM proteins, and this was reported to be a critical step for progression of the fibrosis [3]. The ECM initially accumulates around coronary arteries in response to systemic hypertension and then expands into the interstitial space between *myocardial fibers* [2], therefore suppressing the activation of perivascular fibroblasts might be important to attenuate the adverse remodeling. Using an Ang II-induced hypertensive model, our study supports the previous report by Campbell et al. [7] that Ang II temporally induces the phenotypic change of fibroblasts in the rat heart.

We previously showed that synthetic AM inhibited the Ang II-induced cellular proliferation and growth of cultured cardiac fibroblasts [13]. Consistent with our previous in vitro study [13], we observed in the present study that AM exerted an antiproliferative effect on fibroblasts as determined by the number of Ki-67-positive cells, counteracting the effect of Ang II. In addition, we demonstrated for the first time that the number of adventitial fibroblasts expressing α-SMA, a marker for fibroblast activation, significantly decreased following the AM administration. It should be noted that these AM effects were observed with little change in blood pressure and in left ventricle/body weight and *size of myocardial fiber*. Accordant with the in vitro study by Tomoda et al. [23], cardiac fibroblasts may be more sensitive to AM than *cardiocytes*. Meanwhile, we recently reported using a rat model of myocardial infarction, that AM infusion in an acute phase of the infarction inhibited not only chronic progression of interstitial fibrosis but also of *myocardial* hypertrophy [15]. This seems inconsistent with the present study in terms of alleviation of cardiac hypertrophy; however, the model differs from each other and left ventricular end-diastolic pressure was lowered by the AM infusion in our myocardial infarction experiment. This difference may support the hypothesis for differential regulation of *myocardial* hypertrophy and fibrosis; inappropriate humoral activations stimulate myocardial fibrosis, while hemodynamic factors regulate *growth of myocardial fibers* [2,10,24]. Another possible explanation for the inconsistency may be a difference in the experimental periods of 2 vs. 9 weeks. Because humoral factors including endothelin-1 and TGF-β1 produced by cardiac fibroblasts have been reported to be involved in the *cardiocyte* growth in vitro [25,26], AM treatment for longer periods of time would reduce *growth of myocardial fibers* by modulating fibroblast function.

TGF-β1 plays an important role in myocardial and vascular fibrosis by stimulating the phenotypic change of fibroblasts to myofibroblasts [3] capable of producing matrix proteins. Indeed, blockage of the TGF-β1 action produced the beneficial effect on fibrosis in pressure-overloaded heart [10]. This is comparable with the report by Jesmin et al. [27] showing that the TGF-β1 immunoreactivity is intensely stained in the perivascular area as well as in the vascular wall, concomitantly with TGF-β1 gene up-regulation, in the process of vascular remodeling. In the present study, the reductions of TGF-β1 and type 1 collagen expression with reduced collagen deposition were observed in the AM-treated rats. Both TGF-β1 and AM have been reported to be expressed in a similar pattern during the development of embryonic mouse heart [28] and, in addition, von der Hardt et al. [29] reported that aerosolized AM inhibited TGF-β1 gene expression in the porcine lung. Thus, there seems to be interaction between these two growth-regulatory factors in the process of vascular remodeling.

Many of the AM actions have been shown to be mediated by accumulation of intracellular cyclic AMP (cAMP) [12] and consistent with this, significance of cAMP signaling in attenuating the myofibroblastic change was reported in lung fibroblasts [30] and in hepatic stellate cells [31]. Our in vitro experiments of this study showed that both AM and the cAMP analogue inhibited protein expression of α-SMA induced by TGF-β1 in cultured cardiac fibroblasts; while the protein kinase A inhibition reversed the action of AM. In comparison with the in vivo experiments, the much higher concentration of AM was required to see the clear suppression of α-SMA levels in cultured cardiac fibroblasts; although the present findings suggest possible involvement of the cAMP-protein kinase A pathway in attenuation of the myofibroblast differentiation by AM.

According to the recent reports, heterozygotes of AM knockout mice have shown augmented responses of interstitial or perivascular fibrosis in the myocardium of pressure overload [32] and Ang II/salt-loading hypertension [33] and of intimal hyperplasia in cuff-induced vascular injury [34], compared to their littermates, suggesting cardiovascular protective effects of AM. The proposed mechanisms for such AM effects protective against cardiovascular remodeling are suppression of the renin–angiotensin–aldosterone system and reductions of oxidative stress and protein kinase C activity [15,32–34]. Our present study suggests the profile of AM as an antifibrotic factor counteracting TGF-β1 action by modulating myofibroblast differentiation in the process of vascular remodeling. Meanwhile, Ang II was used to induce hypertension and coronary perivascular fibrosis in the present study, but we are unable to attribute the beneficial effects of AM to specific inhibition of the action of Ang II. These effects may be expected in other forms of hypertension; although further studies are necessary to clarify this point.

In summary, AM infusion for 2 weeks attenuated the Ang II-induced coronary matrix remodeling, suppressing fibroblast activation and expression of TGF-β1 in rats. Because AM is produced in the myocardium and vascular wall, these findings further support the notion that AM is a modulator of cardiovascular remodeling via modulation of fibroblast function.

Acknowledgements

This study was supported by the grants-in-aid for Scientific Research on Priority Areas and for the 21st Century Centers of Excellence Program (Life Science) from the Ministry of Education, Culture, Sport, Science and Technology, Japan, and by a grant-in-aid from AstraZeneca Research 2003. We gratefully thank Ms. Ritsuko Sotomura and Mariko Tokashiki for their technical assistance.

References

[1] Weber KT. Targeting pathological remodeling: concepts of cardioprotection and reparation. Circulation 2000;102:1342–5.
[2] Nicoletti A, Michel JB. Cardiac fibrosis and inflammation: interaction with hemodynamic and hormonal factors. Cardiovasc Res 1999; 41:532–43.
[3] Powell DW, Mifflin RC, Valentich JD, Crowe SE, Saada JI, West AB. Myofibroblasts: I. Paracrine cells important in health and disease. Am J Physiol 1999;277(Cell Physiol 46):C1–9.
[4] Shi Y, O'Brien JE Jr, Fard A, Zalewski A. Transforming growth factor-β1 expression and myofibroblast formation during arterial repair. Arterioscler Thromb Vasc Biol 1996;16:1298–305.
[5] Campbell SE, Katwa LC. Angiotensin II stimulated expression of transforming growth factor-β1 in cardiac fibroblasts and myofibroblasts. J Mol Cell Cardiol 1997;29:1947–58.
[6] McEwan PE, Gray GA, Sherry L, Webb DJ, Kenyon CJ. Differential effects of angiotensin II on cardiac cell proliferation and intramyocardial perivascular fibrosis in vivo. Circulation 1998; 98:2765–73.
[7] Campbell SE, Janicki JS, Weber KT. Temporal differences in fibroblast proliferation and phenotype expression in response to chronic administration of angiotensin II or aldosterone. J Mol Cell Cardiol 1995;27:1545–60.
[8] Lijnen PJ, Petrov VV, Fagard RH. Association between transforming growth factor-β and hypertension. Am J Hypertens 2003;16:604–11.
[9] Wilcox JN, Okamoto EI, Nakahara KI, Vinten-Johansen J. Perivascular responses after angioplasty which may contribute to postangioplasty restenosis: a role for circulating myofibroblast precursors? Ann N Y Acad Sci 2001;947:68–90.
[10] Kuwahara F, Kai H, Tokuda K, Kai M, Takeshita A, Egashira K, et al. Transforming growth factor-β function blocking prevents myocardial fibrosis and diastolic dysfunction in pressure-overloaded rats. Circulation 2002;106:130–5.
[11] Kitamura K, Kangawa K, Kawamoto M, Ichiki Y, Nakamura S, Matsuo H, et al. Adrenomedullin: a novel hypotensive peptide isolated from human pheochromocytoma. Biochem Biophys Res Commun 1993;192:553–60.
[12] Kitamura K, Kangawa K, Eto T. Adrenomedullin and PAMP: discovery, structures, and cardiovascular functions. Microsc Res Tech 2002;57:3–13.
[13] Tsuruda T, Kato J, Kitamura K, Kawamoto M, Kuwasako K, Imamura T, et al. An autocrine or a paracrine role of adrenomedullin in modulating cardiac fibroblast growth. Cardiovasc Res 1999;43:958–67.
[14] Horio T, Nishikimi T, Yoshihara F, Matsuo H, Takishita S, Kangawa K. Effects of adrenomedullin on cultured rat cardiac myocytes and fibroblasts. Eur J Pharmacol 1999;382:1–9.
[15] Nakamura R, Kato J, Kitamura K, Onitsuka H, Imamura T, Cao Y, et al. Adrenomedullin administration immediately after myocardial infarction ameliorates progression of heart failure in rats. Circulation 2004;110:426–31.
[16] Tsuruda T, Jougasaki M, Boerrigter G, Costello-Boerrigter LC, Cataliotti A, Lee SC, et al. Ventricular adrenomedullin is associated with myocyte hypertrophy in human transplanted heart. Regul Pept 2003;112:161–6.
[17] Tsuruda T, Kato J, Kitamura K, Imamura T, Koiwaya Y, Kangawa K, et al. Enhanced adrenomedullin production by mechanical stretching in cultured rat cardiomyocytes. Hypertension 2000;35:1210–4.
[18] Ota T, Takamura T, Ando H, Nohara E, Yamashita H, Kobayashi K. Preventive effect of cerivastatin on diabetic nephropathy through suppression of glomerular macrophage recruitment in a rat model. Diabetologia 2003;46:843–51.
[19] Nishikawa N, Yamamoto K, Sakata Y, Mano T, Yoshida J, Miwa T, et al. Differential activation of matrix metalloproteinases in heart failure with and without ventricular dilatation. Cardiovasc Res 2003;57:766–74.
[20] Proudnikov D, Yuferov V, Zhou Y, LaForge KS, Ho A, Kreek MJ. Optimizing primer-probe design for fluorescent PCR. J Neurosci Methods 2003;123:31–45.
[21] Tsuruda T, Boerrigter G, Huntley BK, Noser JA, Cataliotti A, Costello-Boerrigter LC, et al. Brain natriuretic peptide is produced in cardiac fibroblasts and induces matrix metalloproteinases. Circ Res 2002;91:1127–34.
[22] Zak R. Cell proliferation during cardiac growth. Am J Cardiol 1973;31:211–9.
[23] Tomoda Y, Kikumoto K, Isumi Y, Katafuchi T, Tanaka A, Kangawa K, et al. Cardiac fibroblasts are major production and target cells of adrenomedullin in the heart in vitro. Cardiovasc Res 2001;49:721–30.
[24] Burlew BS, Weber KT. Connective tissue and the heart. Functional significance and regulatory mechanisms. Cardiol Clin 2000; 18:435–42.
[25] Gray MO, Long CS, Kalinyak JE, Li HT, Karliner JS. Angiotensin II stimulates cardiac myocyte hypertrophy via paracrine release of

TGF-β1 and endothelin-1 from fibroblasts. Cardiovasc Res 1998;40: 352–63.
[26] Harada M, Saito Y, Nakagawa O, Miyamoto Y, Ishikawa M, Kuwahara K, et al. Role of cardiac nonmyocytes in cyclic mechanical stretch-induced myocyte hypertrophy. Heart Vessels 1997;12:198–200.
[27] Jesmin S, Sakuma I, Hattori Y, Kitabatake A. Role of angiotensin II in altered expression of molecules responsible for coronary matrix remodeling in insulin-resistant diabetic rats. Arterioscler Thromb Vasc Biol 2003;23:2021–6.
[28] Montuenga LM, Mariano JM, Prentice MA, Cuttitta F, Jakowlew SB. Coordinate expression of transforming growth factor-β1 and adrenomedullin in rodent embryogenesis. Endocrinology 1998;139:3946–57.
[29] von der Hardt K, Kandler MA, Popp K, Schoof E, Chada M, Rascher W, et al. Aerosolized adrenomedullin suppresses pulmonary transforming growth factor-β1 and interleukin-1β gene expression in vivo. Eur J Pharmacol 2002;457:71–6.
[30] Kolodsick JE, Peters-Golden M, Larios J, Toews GB, Thannickal VJ, Moore BB. Prostaglandin E_2 inhibits fibroblast to myofibroblast transition via E. prostanoid receptor 2 signaling and cyclic adenosine monophosphate elevation. Am J Respir Cell Mol Biol 2003;29:537–44.
[31] Mallat A, Préaux AM, Serradeil-Le Gal C, Raufaste D, Gallois C, Brenner DA, et al. Growth inhibitory properties of endothelin-1 in activated human hepatic stellate cells: a cyclic adenosine monophosphate-mediated pathway. Inhibition of both extracellular signal-regulated kinase and c-Jun kinase and upregulation of endothelin B receptors. J Clin Invest 1996;98:2771–8.
[32] Niu P, Shindo T, Iwata H, Iimuro S, Takeda N, Zhang Y, et al. Protective effects of endogenous adrenomedullin on cardiac hypertrophy, fibrosis, and renal damage. Circulation 2004;109:1789–94.
[33] Shimosawa T, Shibagaki Y, Ishibashi K, Kitamura K, Kangawa K, Kato S, et al. Adrenomedullin, an endogenous peptide, counteracts cardiovascular damage. Circulation 2002;105:106–11.
[34] Kawai J, Ando K, Tojo A, Shimosawa T, Takahashi K, Onozato ML, et al. Endogenous adrenomedullin protects against vascular response to injury in mice. Circulation 2004;109:1147–53.

Available online at www.sciencedirect.com

SCIENCE DIRECT

European Journal of Pharmacology 508 (2005) 201–204

www.elsevier.com/locate/ejphar

Adrenomedullin alleviates not only neointimal formation but also perivascular hyperplasia following arterial injury in rats

Toshihiro Tsuruda[a,b,*], Johji Kato[a], Eizaburo Matsui[a], Kinta Hatakeyama[c], Hiroyuki Masuyama[a], Takuroh Imamura[a], Kazuo Kitamura[a], Yujiro Asada[c], Tanenao Eto[a]

[a]*First Department of Internal Medicine, Miyazaki Medical College, University of Miyazaki, Japan*
[b]*Department of Nutrition Management, Faculty of Health and Nutrition, Minami-Kyushu University, Japan*
[c]*First Department of Pathology, Miyazaki Medical College, University of Miyazaki, Japan*

Received 19 August 2004; received in revised form 11 November 2004; accepted 10 December 2004
Available online 7 January 2005

Abstract

Producing components of the extracellular matrix, the vascular adventitia has been recognized as an important modulator of the vascular remodeling process, which determines the vessel architecture. In this study, we examined the effect of the vasodilator peptide adrenomedullin on vascular remodeling induced by balloon injury of rat carotid arteries. Endothelial denudation with wall stretch by ballooning not only induced neointimal formation accompanied with a reduced ratio of the lumen to vessel area, but also increased the fibroblast number and collagen deposition in the adventitial layer. When compared with the saline infusion, intravenous adrenomedullin infusion at 200 ng/h for 14 days suppressed the neointimal formation (−33%, P=0.033), reversing the ratio of lumen to vessel ratio (P=0.030), without affecting systolic blood pressure. Moreover, the adrenomedullin infusion decreased the number of adventitial fibroblasts (−41%, P<0.001) and the collagen deposition (−36%, P=0.006) in the adventitial layer of the injured artery. In conclusion, the intravenous adrenomedullin infusion effectively attenuates vascular remodeling following the arterial injury via suppression of hyperplasia in the intima and adventitia, suggesting a potential of adrenomedullin as a therapeutic tool against vascular remodeling.

Keywords: Remodeling; Extracellular matrix; Adventitia

1. Introduction

Arterial remodeling is a physiological and pathological reaction in response to hemodynamic, immunologic, and biochemical stimuli (Pasterkamp et al., 2004). Medial hypertrophy and neointimal lesion were focused on as important features; however recent studies have concentrated on reorganization of the entire vessel architecture as vascular remodeling (Strauss and Rabinovitch, 2000; Ward et al., 2000). Accumulating evidence suggests an importance for the adventitial layer, which modulate the remodeling process through regulation of the extracellular matrix formation (Sartore et al., 2001; Strauss and Rabinovitch, 2000). A rodent model of arterial balloon injury is widely used to examine the remodeling process due to its similarity to restenotic vascular lesions seen after angioplasty in humans (De Meyer and Bult, 1997). In this model, the vascular injuries cause proliferation and migration of vascular smooth muscle cells (VSMC) into the intima, and fibroblasts increase in cell number, along with an increase in extracellular matrix deposition in the adventitial layer, further aggravating vascular remodeling (Sartore et al., 2001; Ryan et al., 2003). Various humoral interactions between growth factors, inflammatory cytokines or vasoactive peptides have been reported to be involved in the remodeling process (Sartore et al., 2001). Adrenomedullin, initially isolated from human pheochromocytoma (Kitamura et al., 1993), has been shown to have multiple functions in the cardiovascular system (Kitamura

* Corresponding author. First Department of Internal Medicine, Miyazaki Medical College, University of Miyazaki, 5200 Kihara Kiyotake, Miyazaki 889-1692, Japan. Tel.: +81 985 85 0872; fax: +81 985 85 6596.
E-mail address: ttsuruda@med.miyazaki-u.ac.jp (T. Tsuruda).

0014-2999/$ - see front matter © 2004 Elsevier B.V. All rights reserved.
doi:10.1016/j.ejphar.2004.12.019

et al., 2002). Adrenomedullin was shown to inhibit the migration and proliferation of VSMC in vitro (Kano et al., 1996; Kohno et al., 1997), and Agata et al. (2003) reported that adrenomedullin gene delivery produced an inhibitory action on neointima formation after balloon injury, suggesting an important role for this bioactive peptide in vascular remodeling. However, it remains unknown whether the adrenomedullin actions are observed only in the vascular intimal layer or in the whole vascular structure in the remodeling process. The aim of the present study was to examine the biological actions of adrenomedullin on vascular remodeling, which includes not only the neointima formation but also the adventitia hyperplasia in balloon-injured carotid arteries of rats.

2. Materials and methods

The present study was performed in accordance with the Animal Welfare Act and with approval of the University of Miyazaki Institutional Animal Care and Use Committee (2003-023).

2.1. Experimental protocol

Ten- to eleven-week-old male Sprague-Dawley rats (CLEA, Japan, Inc.) weighing 350–400 g were housed in a temperature- and light-controlled room (25±1 °C; 12/12-h light/dark cycle) with normal rat chow and water given ad libitum. After the rats were anesthetized with 40 mg/kg i.p. of pentobarbital sodium, endothelial denudation and wall stretch of the left common carotid artery were carried out by three passages of a Fogarty 2F balloon catheter (Baxter International, Deerfield, IL, USA). Then, the rats were randomly divided into two groups infused with saline (n=9) or with synthetic rat adrenomedullin (Peptide Institute, Osaka, Japan) at 200 ng/h (n=6) over 14 days. Immediately after the balloon injury, miniosmotic pumps (Alzet model 2002) were implanted subcutaneously to release either saline or adrenomedullin into the right external jugular vein. Blood pressure was monitored by tail-cuff plethysmography during the experimental period. At day 14, the rats were anesthetized with 40 mg/kg i.p. of pentobarbital sodium and blood samples were collected from the inferior vena cava. Both the injured left common carotid artery and non-injured contralateral were perfused via the left ventricle with phosphate buffer-saline, followed by perfusion fixation with 4% paraformaldehyde, at the physiological constant pressure of about 100 mm Hg, and were then immediately excised.

2.2. Histology and morphological evaluation

The carotid arteries embedded in paraffin were sectioned at 2 μm thickness. After deparaffinization with xylene and graded alcohol, slides were incubated with 0.1% picrosirius red (Direct Red 80, Sigma) dissolved in saturated picric acid for 10 min. Morphological evaluation of the injured and contralateral uninjured carotid arteries was performed at the middle portion of the artery by a single observer in a blind manner. Two samples were too disfigured to be precisely quantified: one was an injured artery of the control and the other was an intact artery of the adrenomedullin group. Therefore, these two samples were excluded from the analysis. The cross-sectional areas of the lumen and those circumscribed by the internal or external elastic lamina were determined by computerized measurement (Axio Vison 2.05 Carl ZEISS, Munchen, Germany), and the areas of the media and intima were calculated by subtraction. The vessel area was defined as the area surrounded by the external elastic lamina. The number of fibroblasts showing a typical spindle shape in the adventitia was determined at a magnification of ×400. To quantify collagen deposition in the vascular wall, sections stained with picrosirius red were scanned by Mac Scope (v. 2.3.2) software under polarized light. The tightly packed collagen surrounding the carotid artery was defined as the collagen deposition in this study.

2.3. Assay for adrenomedullin

Plasma concentrations of rat adrenomedullin were measured with a specific radioimmunoassay, which detects the C-terminal amide structure of adrenomedullin, an essential portion for the biological activity, as previously described (Tsuruda et al., 1999).

2.4. Statistical analysis

All data are expressed as means±S.E.M. Comparisons between groups were made with one-way analysis of variance followed by the Fisher's test, and statistical significance was accepted at $P<0.05$.

3. Results

3.1. Plasma level of rat adrenomedullin and blood pressure

The adrenomedullin-supplemented rats showed significantly higher rat adrenomedullin levels in the plasma compared with those administered with saline at day 14 (adrenomedullin group, 4.9±0.5; saline group, 3.3±0.2 fmol/ml; P=0.004). Meanwhile, no significant difference in systolic blood pressure was noted before and during the experiment period (data not shown).

3.2. Effects adrenomedullin on neointimal formation and adventitia hyperplasia

Fig. 1 illustrates the hematoxylin-eosin stainings of the intact and balloon-injured carotid arteries at day 14. In the injured artery (B), neointima formation occurred and the

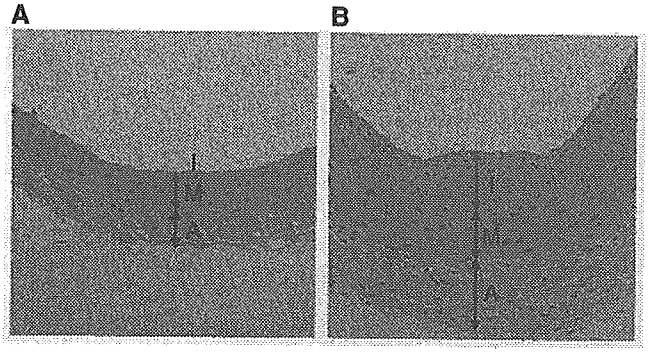

Fig. 1. Histological findings of the intact (A) and injured (B) arteries. I, intima; M, media; A, adventitia. Original magnification, ×200.

adventitial layer thickened with high cellularity, compared with the intact artery (A).

In the quantitative analysis (Fig. 2), the injured arteries showed significant neointimal formation ($P<0.001$) with little influence on the medial area (A) resulting in a significant increase of the intima to media ratio (B). As shown, the adrenomedullin infusion for 14 days significantly attenuated the neointimal formation by 33% ($P=0.033$) and the intima to media ratio by 34% ($P=0.025$), respectively, compared with the saline infusion, while adrenomedullin had no effect on these parameters in the contralateral, intact artery.

Fig. 3A illustrates the effect of adrenomedullin on cell number of fibroblasts in the adventitial layer. The arterial injury increased the number of fibroblasts ($P<0.001$), but this increase was suppressed by the adrenomedullin infusion by 41% ($P<0.001$). Fig. 3B shows the effect of adrenomedullin on the ratio of collagen deposition to the medial areas in the intact and injured arteries. The balloon injury enlarged the collagen deposition area mainly in the adventitia ($P<0.001$); however, the adrenomedullin infusion reduced it by 38% ($P=0.006$).

3.3. Effect of adrenomedullin on geometrical changes in the carotid arteries

Fig. 4A and B illustrate the effect of adrenomedullin on the lumen and vessel areas, respectively. The balloon injury slightly reduced the lumen area of rats infused with saline,

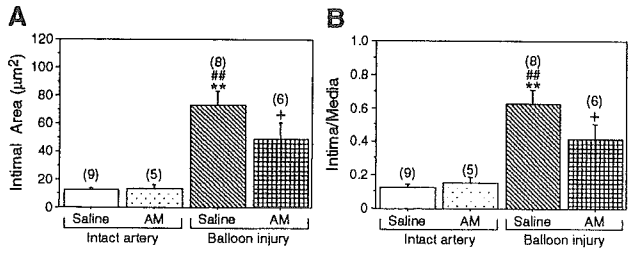

Fig. 2. Effect of adrenomedullin on intimal area (A) and ratio of intima to media (B) in the intact and injured arteries. Values are means±S.E.M., (*n*). **$P<0.01$ vs. intact artery with saline infusion; $^{\#\#}P<0.01$ vs. intact artery with adrenomedullin infusion; $^{+}P<0.05$ vs. injured artery with saline infusion.

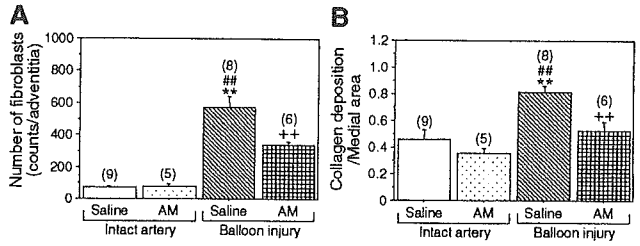

Fig. 3. Effect of adrenomedullin on cell number in the adventitia (A) and collagen deposition/medial area (B). Values are means±S.E.M., (*n*). **$P<0.01$ vs. intact artery with saline infusion; $^{\#\#}P<0.01$ vs. intact artery with adrenomedullin infusion; $^{++}P<0.01$ vs. injured artery with saline infusion.

but this reduction was statistically insignificant (Fig. 4A), and no significant differences were noted in the vessel area of four study groups (Fig. 4B). As shown in Fig. 4C, the ratio of the lumen to vessel area was significantly ($P<0.001$) reduced by the balloon injury in the saline group, compared with those of the intact arteries. The adrenomedullin supplement significantly ($P=0.030$) reversed this geometrical change toward those of the intact arteries.

4. Discussion

We report here that intravenous adrenomedullin infusion not only attenuated neointima formation but also inhibited fibroblast proliferation and collagen deposition of the adventitia, reducing the ratio of lumen to vessel area, in the balloon-injured carotid arteries of rats. The three layers of the vascular wall, intima, media and adventitia, contribute to inward or outward remodeling which occurs following arterial injury (Ward et al., 2000). Although neointimal formation and medial hypertrophy have been focused on as targets in preventing adverse remodeling, recent reports have

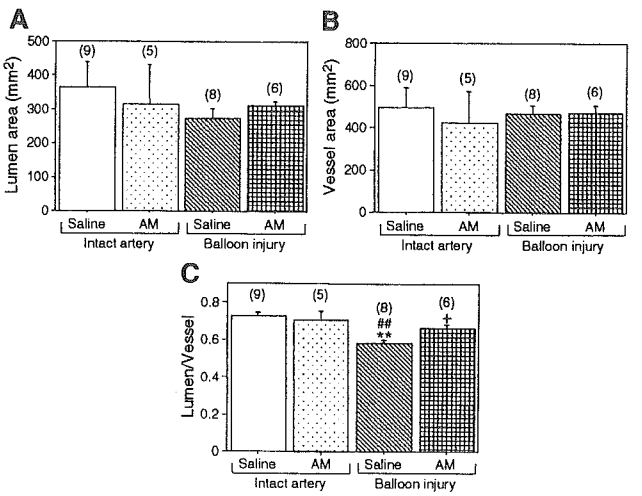

Fig. 4. Effect of adrenomedullin on lumen area (A), vessel area (B) and ratio of lumen to vessel area (C). Values are means±S.E.M., (*n*). **$P<0.01$ vs. intact artery with saline infusion; $^{\#\#}P<0.01$ vs. intact artery with adrenomedullin infusion; $^{+}P<0.05$ vs. injured artery with saline infusion.

referred more to the role of the adventitial layer (Ryan et al., 2003; Sartore et al., 2001; Strauss and Rabinovitch, 2000).

In a model of arterial injury, endothelial denudation induces VSMC proliferation and migration, making up the neointima formation. Our present data supports previous studies showing that adrenomedullin attenuated the neointima formation induced by arterial injuries in rats (Agata et al., 2003; Yamasaki et al., 2003) and in mice (Imai et al., 2002; Kawai et al., 2004). On the other hand, extracellular matrix deposition in the adventitia with cellular hyperplasia appears to be the major phenomena responsible for adventitial thickening that would subsequently increase stiffness of the vascular walls and peripheral arterial resistance (Intengan and Schiffrin, 2001; Sartore et al., 2001). Importantly, we found that the adrenomedullin administration significantly decreased the number of fibroblasts in the adventitia following the arterial injury in this study. In addition, the adrenomedullin-treated rats showed a significant reduction of collagen deposition in the entire vessel wall, mainly in the adventitia. Considering the importance of extracellular matrix formation in determining stiffness of the vascular wall (Intengan and Schiffrin, 2001), adrenomedullin may exert a beneficial action alleviating vascular stiffness.

In this study, the beneficial effects of adrenomedullin following arterial injury were observed without a significant effect on blood pressure, suggesting a direct action of adrenomedullin on the vascular remodeling. Adrenomedullin has been shown to directly inhibit proliferation and migration of cultured VSMC (Kano et al., 1996; Kohno et al., 1997), and according to our previous report (Tsuruda et al., 1999), adrenomedullin inhibited proliferation of cultured fibroblasts isolated from rat cardiac ventricle. Recently, we reported that adrenomedullin induced matrix metalloproteinase-2 activity in cultured adventitial fibroblasts isolated from rat aorta (Tsuruda et al., 2004). Collagen accumulation is responsible for constrictive remodeling following balloon injury (Ryan et al., 2003). Proteolytic activity induced by adrenomedullin may have contributed to attenuating collagen deposition, however these hypotheses for possible, direct actions of adrenomedullin should be tested in vivo by future experiments.

In summary, the intravenous adrenomedullin infusion effectively improves the vascular geometry of the balloon-injured rat carotid artery, suppressing neointima formation, adventitial fibroblast proliferation and collagen deposition. This study implies a possible utility of adrenomedullin for inhibition of vascular remodeling, where both neointimal formation and adventitial hyperplasia are targeted.

Acknowledgements

This study was supported by the grants-in-aid for Scientific Research and for the 21st Century Centers of Excellence Program (Life Science) from the Ministry of Education, Culture, Sport, Science and Technology, Japan, and by a grant -in-aid from AstraZeneca Research 2003. We gratefully thank Ms. Ritsuko Sotomura for her technical assistance.

References

Agata, J., Zhang, J.J., Chao, J., Chao, L., 2003. Adrenomedullin gene delivery inhibits neointima formation in rat artery after balloon angioplasty. Regul. Pept. 112, 115–120.

De Meyer, G.R., Bult, H., 1997. Mechanisms of neointima formation—lessons from experimental models. Vasc. Med. 2, 179–189.

Imai, Y., Shindo, T., Maemura, K., Sata, M., Saito, Y., Kurihara, Y., Akishita, M., Osuga, J., Ishibashi, S., Tobe, K., Morita, H., Oh-hashi, Y., Suzuki, T., Maekawa, H., Kangawa, K., Minamino, N., Yazaki, Y., Nagai, R., Kurihara, H., 2002. Resistance to neointimal hyperplasia and fatty streak formation in mice with adrenomedullin overexpression. Arterioscler. Thromb. Vasc. Biol. 22, 1310–1315.

Intengan, H.D., Schiffrin, E.L., 2001. Vascular remodeling in hypertension. Roles of apoptosis, inflammation, and fibrosis. Hypertension 38, 581–587.

Kano, H., Kohno, M., Yasunari, K., Yokokawa, K., Horio, T., Ikeda, M., Minami, M., Hanehira, T., Takeda, T., Yoshikawa, J., 1996. Adrenomedullin as a novel antiproliferative factor of vascular smooth muscle cells. J. Hypertens. 14, 209–213.

Kawai, J., Ando, K., Tojo, A., Shimosawa, T., Takahashi, K., Onozato, M.L., Yamasaki, M., Ogita, T., Nakaoka, T., Fujita, T., 2004. Endogenous adrenomedullin protects against vascular response to injury in mice. Circulation 109, 1147–1153.

Kitamura, K., Kangawa, K., Kawamoto, M., Ichiki, Y., Nakamura, S., Matsuo, H., Eto, T., 1993. Adrenomedullin: a novel hypotensive peptide isolated from human pheochromocytoma. Biochem. Biophys. Res. Commun. 192, 553–560.

Kitamura, K., Kangawa, K., Eto, T., 2002. Adrenomedullin and PAMP: discovery, structures, and cardiovascular functions. Microsc. Res. Tech. 57, 3–13.

Kohno, M., Yokokawa, K., Kano, H., Yasunari, K., Minami, M., Hanehira, T., Yoshikawa, J., 1997. Adrenomedullin is a potent inhibitor of angiotensin II-induced migration of human coronary artery smooth muscle cells. Hypertension 29, 1309–1313.

Pasterkamp, G., Galis, Z.S., de Kleijn, D.P., 2004. Expansive arterial remodeling: location, location, location. Arterioscler. Thromb. Vasc. Biol. 24, 650–657.

Ryan, S.T., Koteliansky, V.E., Gotwals, P.J., Lindner, V., 2003. Transforming growth factor-beta-dependent events in vascular remodeling following arterial injury. J. Vasc. Res. 40, 37–46.

Sartore, S., Chiavegato, A., Faggin, E., Franch, R., Puato, M., Ausoni, S., Pauletto, P., 2001. Contribution of adventitial fibroblasts to neointima formation and vascular remodeling: from innocent bystander to active participant. Circ. Res. 89, 1111–1121.

Strauss, B.H., Rabinovitch, M., 2000. Adventitial fibroblasts: defining a role in vessel wall remodeling. Am. J. Respir. Cell Mol. Biol. 22, 1–3.

Tsuruda, T., Kato, J., Kitamura, K., Kawamoto, M., Kuwasako, K., Imamura, T., Koiwaya, Y., Tsuji, T., Kangawa, K., Eto, T., 1999. An autocrine or a paracrine role of adrenomedullin in modulating cardiac fibroblast growth. Cardiovasc. Res. 43, 958–967.

Tsuruda, T., Kato, J., Cao, Y.N., Hatakeyama, K., Masuyama, H., Imamura, T., Kitamura, K., Asada, Y., Eto, T., 2004. Adrenomedullin induces matrix metalloproteinase-2 activity in rat aortic adventitial fibroblasts. Biochem. Biophys. Res. Commun. 325, 80–84.

Yamasaki, M., Kawai, J., Nakaoka, T., Ogita, T., Tojo, A., Fujita, T., 2003. Adrenomedullin overexpression to inhibit cuff-induced arterial intimal formation. Hypertension 41, 302–307.

Ward, M.R., Pasterkamp, G., Yeung, A.C., Borst, C., 2000. Arterial remodeling. Mechanisms and clinical implications. Circulation 102, 1186–1191.

0013-7227/05/$15.00/0
Printed in U.S.A.

Endocrinology 146(1):355–364

doi: 10.1210/en.2004-0629

Transgenic Mice Overexpressing Des-Acyl Ghrelin Show Small Phenotype

Hiroyuki Ariyasu, Kazuhiko Takaya, Hiroshi Iwakura, Hiroshi Hosoda, Takashi Akamizu, Yuji Arai, Kenji Kangawa, and Kazuwa Nakao

Department of Medicine and Clinical Science (H.A., K.N.), Kyoto University Graduate School of Medicine, and Translational Research Center (K.T., H.I., H.H., T.A., K.K.), Kyoto University Hospital, Kyoto 606-8507; and Departments of Bioscience (Y.A.) and Biochemistry (K.K.), National Cardiovascular Center Research Institute, Osaka 565-8565, Japan

Ghrelin, a 28-amino acid acylated peptide, displays strong GH-releasing activity in concert with GHRH. The fatty acid modification of ghrelin is essential for the actions, and des-acyl ghrelin, which lacks the modification, has been assumed to be devoid of biological effects. Some recent reports, however, indicate that des-acyl ghrelin has effects on cell proliferation and survival. In the present study, we generated two lines of transgenic mice bearing the preproghrelin gene under the control of chicken β-actin promoter. Transgenic mice overexpressed des-acyl ghrelin in a wide variety of tissues, and plasma des-acyl ghrelin levels reached 10- and 44-fold of those in control mice. They exhibited lower body weights and shorter nose-to-anus lengths, compared with control mice. The serum GH levels tended to be lower, and the serum IGF-I levels were significantly lower in both male and female transgenic mice than control mice. The responses of GH to administered GHRH were normal, whereas those to administered ghrelin were reduced, especially in female transgenic mice, compared with control mice. These data suggest that overexpressed des-acyl ghrelin may modulate the GH-IGF-I axis and result in small phenotype in transgenic mice. (*Endocrinology* 146: 355–364, 2005)

GHRELIN, AN ACYLATED peptide of 28 amino acids, was identified as an endogenous ligand for the GH secretagogue (GHS) receptor (GHS-R) (1). The major site of production of ghrelin is the stomach and it is also expressed in the hypothalamus (2–5). Plasma ghrelin levels are regulated by acute feeding states. They rise by fasting and are rapidly suppressed by feeding (3, 6–8). Secretion of ghrelin is also regulated by chronic feeding states. Plasma ghrelin levels are elevated in patients with anorexia nervosa and food-restricted animals and are reduced in obese subjects (3, 6–10). These data suggest the possible involvement of ghrelin in energy homeostasis. In fact, ghrelin stimulates food intake in animals and humans and exhibits anticachectic effect in cancer-bearing mice (8, 11–13).

Exogenously administered ghrelin strongly stimulates GH release in a clear dose-dependent manner *in vivo* (1, 2, 14–16). The site of ghrelin action on GH release is not well known to date. The GHS-R is reported to be expressed in the pituitary as well as hypothalamus (17–19). Previous studies indicate that ghrelin binds to membranes from the pituitary and stimulates GH release from cultured pituitary cells (1, 20), suggesting that the pituitary is one of the sites of ghrelin actions. The stimulatory effect of GHSs and ghrelin on GH secretion, however, is more prominent *in vivo* than *in vitro*, and intact GHRH signaling is essential for the effect (1, 21). Hexarelin, one of the potent GHSs, cannot efficiently stimulate GH release in patients with GHRH receptor deficiency (22). Moreover, as we demonstrated, ghrelin has a synergistic action with GHRH. Even a low dose of ghrelin can highly augment GH release by GHRH (23). These data indicate a critical role of the hypothalamus in the stimulatory effect of ghrelin on GH secretion. The strong potency of ghrelin suggests its role as a physiological regulator of GH secretion (1, 2, 14–16). The issue, however, is currently controversial. One recent study (24), using a GHS antagonist, revealed that circulating ghrelin in peripheral blood may not play a role in generating pulsatile GH secretion. Moreover, deletion of ghrelin impairs neither growth nor appetite, indicating that ghrelin is not critically required for GH secretion (25). Another study (26), however, demonstrated that the attenuation of the GHS-R expression *in vivo* results in reduction in food intake and growth, suggesting a physiological role of the ghrelin-GHS-R system in the secretory regulation of GH.

The acylation of ghrelin is assumed to be essential for its actions (1). Des-acyl ghrelin, which lacks the fatty acid modification and circulates at 10-fold higher concentration than acylated ghrelin (1, 3, 27), is devoid of any endocrine activities including GH release, based on previous studies (1, 28). Recent studies (29, 30), however, indicated that des-acyl ghrelin may share with acylated ghrelin the modulation of neoplastic cell proliferation and cardiovascular cell survival *in vitro*. Moreover, one study shows that des-acyl ghrelin may offset the inhibitory effect of acylated ghrelin on insulin secretion (28). Although previous studies indicated that several tissues and cell lines produce des-acyl and/or acylated ghrelin (3, 27, 31, 32), the mechanism by which ghrelin is acylated is also unknown to date.

In the present study, we generated transgenic mice bearing the preproghrelin gene under the control of a cytomegalovirus immediate early enhancer and a modified chicken β-

First Published Online October 7, 2004

Abbreviations: BMI, Body mass index; GHS, GH secretagogue; GHS-R, GHS receptor.

Endocrinology is published monthly by The Endocrine Society (http://www.endo-society.org), the foremost professional society serving the endocrine community.

actin promoter, designated CAG promoter (33, 34). This promoter sequence has been demonstrated to have high activity in cultured cells and transgenic mice (33, 34). Transgenic mice in the present study overexpressed des-acyl ghrelin in plasma and a wide variety of tissues and showed small phenotype. Here we show that des-acyl ghrelin may modulate endogenous ghrelin action and alter the GH-IGF-I axis in transgenic mice.

Materials and Methods

All procedures in animal experiments were approved by the Kyoto University Graduate School of Medicine Committee on Animal Research. The procedures were performed in accordance with the principle and guidelines established by the committee.

Plasmid construction and generation of transgenic mice

The full-length mouse preproghrelin cDNA (1) and the pCAGGS expression vector including the CAG promoter (34) were kindly donated by Professor Masayasu Kojima (Division of Molecular Genetics, Institute of Life Science, Kurume University, Kurume, Japan) and Professor Junichi Miyazaki (Department of Nutrition and Physiological Chemistry, Osaka University School of Medicine, Osaka, Japan), respectively. Plasmid pCAGGS-ghrelin was constructed by inserting the mouse preproghrelin cDNA into the unique *Eco*RI site between the CAG promoter and 3′-flanking sequence of the rabbit β-globin gene of the pCAGGS expression vector. The DNA fragment was excised from its plasmid by digestion with *Sal*I and *Hind*III and then purified and microinjected into the pronuclei of fertilized eggs obtained from BDF1 female mice (Charles River Japan, Yokohama, Japan) as reported previously (35). Founder transgenic mice were identified by PCR analysis and bred with C57BL/6 mice (Japan CLEA, Osaka, Japan). Mice were housed in air-conditioned animal quarters, with the lights on between 0800 and 2000 h and were given standard rat chow (CE-2, 352 kcal per 100 g, Japan CLEA) and water *ad libitum*.

Measurement of total and acylated ghrelin levels in tissue samples

Tissues such as the stomach, cerebrum, heart, and kidney were removed from 8-wk-old mice under anesthesia with diethyl ether. Each sample was diced and boiled for 7 min in a 5-fold volume of water. The solution was adjusted to 1.0 M acetic acid and 20 mM hydrogen chloride after boiling, and the tissue was homogenized. The supernatant was obtained after centrifugation at 10,000 rpm for 30 min. Tissue ghrelin levels were measured using two kinds of RIAs, C-RIA for the carboxyl terminal and N-RIA for the amino terminal of ghrelin as reported previously (9, 27). C-RIA and N-RIA recognize total (acylated plus des-acyl ghrelin) and acylated ghrelin, respectively (9, 27).

Measurement of plasma total and acylated ghrelin levels

Blood samples were collected from the inferior vena cava of mice under anesthesia with diethyl ether. The samples were immediately transferred to chilled polypropylene tubes containing Na_2EDTA (1 mg/ml) and aprotinin (Ohkura Pharmaceutical, Inc., Kyoto, Japan; 1000 kallikrein inactivator U/ml) and centrifuged at 4 C. For N-RIA, hydrogen chloride was added to the samples at final concentration of 0.1 N immediately after the separation of plasma. Plasma ghrelin was measured as reported previously (1, 3, 27). Briefly, the samples were subjected to a Sep-Pak C18 cartridge and C-RIA and N-RIA were carried out.

Measurement of body weights and lengths, organ weights, and daily food intake

Body weights of control and transgenic mice were measured weekly, beginning at 3 wk of age. Body lengths of 8- and 52-wk-old mice were measured by manual immobilization and extension of mice to the nose-to-anus lengths, always by the same individual. Body mass indexes (BMIs = weight/(nose-to-anus lengths)^2) were calculated in 8- and 52-wk-old control and transgenic mice (36, 37). Organs such as the pituitary, stomach, cerebrum, heart, liver, kidney, spleen, pancreas, and epididymal fat were removed from 8-wk-old mice under anesthesia with diethyl ether and weighed. Daily food intake was monitored for 3 wk, beginning at 5 wk of age.

Measurement of blood glucose, serum total protein, total cholesterol, and hormones

To examine the nutritional conditions, blood glucose and serum total protein and total cholesterol levels were measured. Eight-week-old control and transgenic mice were used. Four hundred microliters of blood samples were collected from the tail vein of mice for blood glucose levels at 1000 h after 12 h fasting. Then the mice were anesthetized with diethyl ether, and 400 μl of blood samples were collected from the inferior vena cava for serum total protein, total cholesterol, and hormone levels. Blood glucose, serum total protein, and total cholesterol levels were measured by the glucose oxidase method with a reflectance glucometer (One Touch II; Lifescan, Milpitas, CA), BCA protein assay reagent kit (Pierce, Rockford, IL), and Amplex red cholesterol assay kit (Molecular Probes, Eugene, OR), respectively. Serum GH and IGF-I levels were measured with EIA kits (SPI-BIO, Bonde, France, and Diagnostic Systems Laboratories Inc., Webster, TX, respectively). Serum insulin and plasma ACTH levels were measured with EIA kits (Morinaga, Tokyo, Japan) and ACTH-RIA kit (Nichols Institute Diagnostics, San Juan Capistrano, CA), respectively. Serum TSH, LH, and FSH levels were measured with EIA kits (Amersham Biosciences, Buckinghamshire, UK).

Effects of GHRH and ghrelin on serum GH levels

Human GHRH and rat ghrelin were purchased from Sumitomo Pharmaceuticals Co., Ltd. (Osaka, Japan) and Peptide Institute, Inc. (Osaka, Japan), respectively. Male and female 8-wk-old control and Tg 10–1 mice were used under no anesthesia. Control and transgenic mice were housed in the same cage and tested on the same day. Forty mice were divided into five groups for blood sampling. Eight mice in the same group were used for each blood sampling. Control and transgenic mice were iv injected with human GHRH (60 μg/kg) or rat ghrelin (40 μg/kg). Four hundred microliters of blood samples were collected from the inferior vena cava of mice 0, 10, 20, 30, and 60 min after the injection. Serum GH levels were measured with an EIA kit (SPI-BIO).

Real-time PCR analysis of preproghrelin, GH, GHRH, somatostatin, and GHS-R mRNAs

Total RNAs from tissues, such as the stomach, small intestine, cerebrum, hypothalamus, pituitary, liver, kidney, lung, heart, and skeletal muscle, were extracted using the acid guanidinium thiocyanate-phenol-chloroform method (38). First-strand cDNA was synthesized from 1 μg of total RNA using Superscript II RT (Life Technologies, Inc., St. Louis, MO) with random hexamers according to the manufacturer's instructions. Taqman-PCR was performed with the ABI Prism 7700 sequence detection system (Applied Biosystems, Foster City, CA) using VIC-labeled fluorogenic probes specific for preproghrelin, GH, GHRH, somatostatin, or GHS-R transcript, or the internal standard glyceraldehyde-3-phosphate dehydrogenase. Oligo primers and probes (Table 1) were chosen using the Primer Express software (Applied Biosystems). The PCR was performed using Taqman Universal PCR Mastermix (Applied Biosystems) to which primers and probes were added (final concentrations 400 and 200 nM, respectively). All samples were run in triplicate in 96-well plates in the ABI Prism 7700 sequence detector according to the manufacturer's standard protocol. For the primer sets, serial dilutions were conducted with different cDNA preparations to confirm the kinetics of the PCR. There was no significant difference in glyceraldehyde-3-phosphate dehydrogenase mRNA levels among experimental groups.

Effects of continuous infusion of des-acyl ghrelin on the GH-IGF-I axis and body weights

Rat des-acyl ghrelin was purchased from Peptide Institute, Inc. Des-acyl ghrelin was dissolved in saline at a concentration of 700 μg/ml and stored in osmotic minipumps (DURECT Corp., Cupertino, CA). The

TABLE 1. Primer and probe sequences for real-time PCR analysis for preproghrelin, GH, GHRH, somatostatin, and GHS-R mRNAs

	Primer and probe sequences
Preproghrelin	
Forward	5′-GCATGCTCTGGATGGACATG-3′
Reverse	5′-TGGTGGCTTCTTGGATTCCT-3′
Probe	5′-AGCCCAGAGCACCAGAAAGCCCA-3′
GH	
Forward	5′-AAGAGTTCGAGCGTGCCTACA-3′
Reverse	5′-GAAGCAATTCCATGTCGGTTC-3′
Probe	5′-CCATTCAGAATGCCCAGGCTGCTTTC-3′
GHRH	
Forward	5′-AGGATGCAGCGACACGTAGA-3′
Reverse	5′-TCTCCCCTTGCTTGTTCATGA-3′
Probe	5′-CCACCAACTACAGGAAACTCCTGAGCCA-3′
Somatostatin	
Forward	5′-AGCTGAGCAGGACGAGATGAG-3′
Reverse	5′-ACAGGATGTGAATGTCTTCCAGAA-3′
Probe	5′-CGAACCCAGCAATGGCACCCC-3′
GHS-R	
Forward	5′-CACCAACCTCTACCTATCCAGCAT-3′
Reverse	5′-CTGACAAACTGGAAGAGTTTGCA-3′
Probe	5′-TAAGATCTGCTCATCTTAATGTGCATG-3′

minipumps were implanted into the peritoneum. Des-acyl ghrelin or saline was infused continuously through the minipumps into 4-wk-old C57/BL6 mice (Japan CLEA) for 10 d. The minipumps were continuously delivering saline or 250 μg/kg·d of des-acyl ghrelin for 10 d at a speed of 0.22 μl/h. Body weights were measured daily for 10 d. Four hundred microliters of blood samples for the measurement of serum GH and IGF-1 levels were collected from the inferior vena cava of mice under anesthesia with diethyl ether 10 d after the implantation.

Hematoxylin eosin and immunohistochemical staining for total ghrelin, acylated ghrelin, and GH of the pituitary

The pituitaries were removed from male 8-wk-old mice under anesthesia with diethyl ether and fixed with 4% paraformaldehyde and 0.2% picric acid and embedded in paraffin. The tissues were cut in 3-μm-thick slices. Samples were subjected to immunohistochemical staining for total and acylated ghrelin as well as hematoxylin eosin staining. After pretreatment with 0.3% hydrogen peroxide and incubation with normal goat serum, all slices were incubated overnight at 4 C with ghrelin(13–28) antiserum recognizing total (des-acyl plus acylated) ghrelin (final dilution, 1:5000), antighrelin(1–11) antiserum specifically recognizing acylated ghrelin (final dilution, 1:5000), or anti-GH antiserum (Biogenesis, Poole, UK) (final dilution, 1:200). All of the sections were stained by the avidin-biotin complex method and counterstained with hematoxylin as reported previously (39).

Statistical analysis

Results are expressed as the mean ± SEM. ANOVA followed by the *t* test was used to assess differences between control and transgenic mice. $P < 0.05$ was considered to be statistically significant.

Results

Generation of transgenic mice and preproghrelin mRNA levels

Two lines of transgenic mice with six (Tg 10–1) and 12 (Tg 9–2) copy numbers were identified by PCR and Southern blot analysis. Preproghrelin mRNAs were detected only in the stomach, small intestine, lung, pituitary, and hypothalamus of control mice, and the amounts were 100, 4, 2.1, 1.5, and 0.5 in arbitrary units (AU), respectively (Fig. 1). On the other hand, they were detected in all tissues examined in Tg 9–2 and Tg 10–1 mice, and the amounts in the stomach of Tg 9–2 and Tg 10–1 mice reached 1100 and 5200 AU, respectively (Fig. 1). Preproghrelin mRNA levels in other tissues of Tg 9–2 and Tg 10–1 mice also exceeded those of control mice.

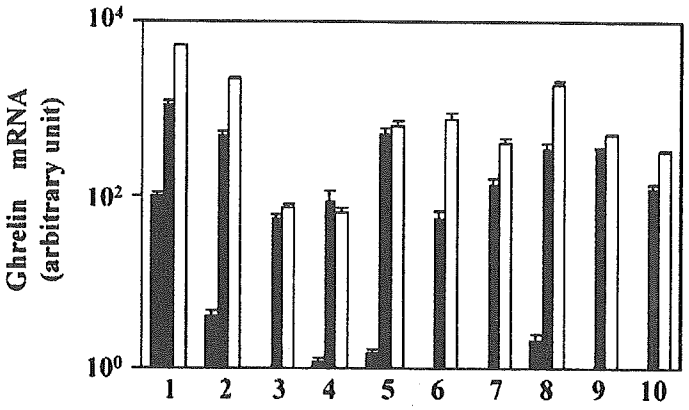

FIG. 1. Preproghrelin mRNA levels in the tissues of control (*closed bars*), Tg 9–2 (*shaded bars*), and Tg 10–1 (*open bars*) mice quantified by real-time PCR analysis. Lanes 1, stomach; 2, small intestine; 3, cerebrum; 4, hypothalamus; 5, pituitary; 6, liver; 7, kidney; 8, lung; 9, heart; and 10, skeletal muscle.

Total and acylated ghrelin levels in tissues and plasma

Eight-week-old control, Tg 9–2, and Tg 10–1 mice were used (Table 2). Although high total ghrelin levels were detected in the stomach, only very low levels were detected in other tissues of control mice. Tg 9–2 and Tg 10–1 mice showed significantly higher total ghrelin levels in the stomach than control mice ($P < 0.01$ for each). Tg 9–2 and Tg 10–1 mice also showed total ghrelin levels in all of the other tissues significantly higher than control mice. High levels of acylated ghrelin were also detected in the stomach of control, Tg 9–2, and Tg 10–1 mice. There was, however, no significant difference between control and Tg 9–2 mice and between control and Tg 10–1 mice. Only very low acylated ghrelin levels if any were detected in other tissues of control, Tg 9–2, and Tg 10–1 mice. Plasma total ghrelin levels in control, Tg 9–2, and Tg 10–1 mice were 1104.5 ± 94.4, 11230.6 ± 1147.1, and 48565.5 ± 9291.5 fmol/ml, respectively. Those in Tg 9–2 and Tg 10–1 mice were significantly higher than those in control mice ($P < 0.01$ for each). Plasma acylated ghrelin levels in control, Tg 9–2, and Tg 10–1 mice were 83.7 ± 11.9, 79.7 ± 10.1, and 86.3 ± 21.1 fmol/ml, respectively. The differences between control and Tg 9–2 mice and control and Tg 10–1 mice were not significant.

Body weights and lengths, relative organ weights, and BMIs

Body weights of control, Tg 9–2, and Tg 10–1 mice are shown in Table 3 and Fig. 2A. Male Tg 9–2 and Tg 10–1 mice were significantly lighter in the body weight than control mice ($P < 0.05$ and $P < 0.01$, respectively). Female Tg 10–1 mice were also significantly lighter than control mice ($P < 0.01$). The difference between female control and Tg 9–2 mice was not significant. Fifteen-week-old male and female Tg 10–1 and male Tg 9–2 mice were still significantly lighter than control mice ($P < 0.05$, $P < 0.01$, and $P < 0.01$, respectively). Body lengths (nose-to-anus lengths) of control and

TABLE 2. Total and acylated ghrelin levels in plasma and tissues of 8-wk-old control and transgenic mice (n = 8/group)

	Control	Tg 9-2	Tg 10-1
Total ghrelin			
Plasma (fmol/ml)	1104.5 ± 94.4	11230.6 ± 1147.1[a]	48565.5 ± 9291.5[a]
Tissues (fmol/mg)			
Stomach	2191.9 ± 340.9	2860.8 ± 587.3[a]	5430.6 ± 626.1[a]
Cerebrum	0.8 ± 0.2	34.3 ± 4.2[a]	110.9 ± 41.0[a]
Heart	1.4 ± 0.2	27.6 ± 5.6[a]	30.2 ± 9.3[a]
Kidney	1.9 ± 0.1	43.5 ± 5.9[a]	68.3 ± 10.5[a]
Acylated ghrelin			
Plasma (fmol/ml)	83.7 ± 11.9	79.7 ± 10.6	86.3 ± 21.1
Tissues (fmol/mg)			
Stomach	413.0 ± 46.7	341.2 ± 66.8	325.0 ± 49.5
Cerebrum	0.05>	0.05>	0.05>
Heart	0.1 ± 0.0	0.05>	0.05>
Kidney	0.1 ± 0.0	0.1 ± 0.1	0.1 ± 0.0

Values are given as the mean ± SEM.
[a] $P < 0.01$ *vs.* control mice.

transgenic mice are shown in Table 3. Eight-week-old male Tg 9–2 and Tg 10–1 mice were significantly shorter in the body length than control mice ($P < 0.05$ and $P < 0.01$, respectively). Female Tg 10–1 mice were significantly shorter than control mice ($P < 0.01$). The difference between female control and Tg 9–2 mice was not significant. BMIs were calculated from the body weights and lengths. No significant difference was noted between control and Tg 9–2 mice and control and Tg 10–1 mice (Table 3). Fifty-two-week-old male Tg 9–2 and Tg10–1 mice were still significantly lighter and shorter, compared with control mice (Table 3), and no significant difference was noted in BMIs between control and transgenic mice. Relative organ weights of 8-wk-old male control and Tg 10–1 mice were calculated from the organ and body weights. No significant difference was noted between control and Tg 10–1 mice (Fig. 2B). No significant difference was noted in the pituitary size between control and Tg 10–1 mice (0.058 ± 0.002 and 0.055 ± 0.003 mg/body weight (grams), respectively).

TABLE 3. Body weights, lengths, and BMIs of 8-wk-old and 52-wk-old control and transgenic mice (n = 8/group)

		Control	Tg 9-2	Tg 10-1
Male				
8-wk-old	Body weight (g)	23.2 ± 0.5	21.0 ± 0.7[a]	16.6 ± 0.6[b]
	Nose-to-anus length (cm)	9.2 ± 0.3	8.6 ± 0.1[a]	7.7 ± 0.3[b]
	BMI (g/cm^2)	27.1 ± 1.2	28.1 ± 3.1[c]	27.3 ± 1.9[c]
52-wk-old	Body weight (g)	34.7 ± 0.8	31.2 ± 0.6[a]	28.4 ± 0.1[b]
	Nose-to-anus length (cm)	10.1 ± 0.1	9.5 ± 0.3[a]	9.1 ± 0.1[b]
	BMI (g/cm^2)	34.4 ± 0.8	34.7 ± 0.6[c]	34.5 ± 0.8[c]
Female				
8-wk-old	Body weight (g)	16.6 ± 1.2	18.7 ± 0.7[c]	10.7 ± 1.1[b]
	Nose-to-anus length (cm)	8.1 ± 0.6	8.5 ± 0.2[c]	6.4 ± 0.2[b]
	BMI (g/cm^2)	25.8 ± 1.8	26.2 ± 1.2[c]	26.5 ± 1.5[c]
52-wk-old	Body weight (g)	25.3 ± 1.3	24.8 ± 0.8[c]	19.6 ± 0.7[b]
	Nose-to-anus length (cm)	9.0 ± 0.4	8.9 ± 0.3[c]	7.9 ± 0.2[b]
	BMI (g/cm^2)	30.9 ± 1.0	31.2 ± 0.7[c]	31.3 ± 1.1[c]

Values are given as the mean ± SEM.
[a] $P < 0.05$ *vs.* control mice.
[b] $P < 0.01$ *vs.* control mice.
[c] Not significant.

Immunohistochemical staining for total and acylated ghrelin of the pituitary

Immunohistochemical staining for total and acylated ghrelin is shown in Fig. 3, A–D. None of total ghrelin-positive cells were observed in the pituitary of control mice (Fig. 3A). On the other hand, many total ghrelin-immunoreactive pituitary cells were observed in Tg 10–1 mice (Fig. 3B). Approximately 30% of the anterior pituitary cells in all sections examined were total ghrelin immunoreactive. None of acylated ghrelin-positive cells were observed in the pituitary of either control or Tg 10–1 mice (Fig. 3, C and D).

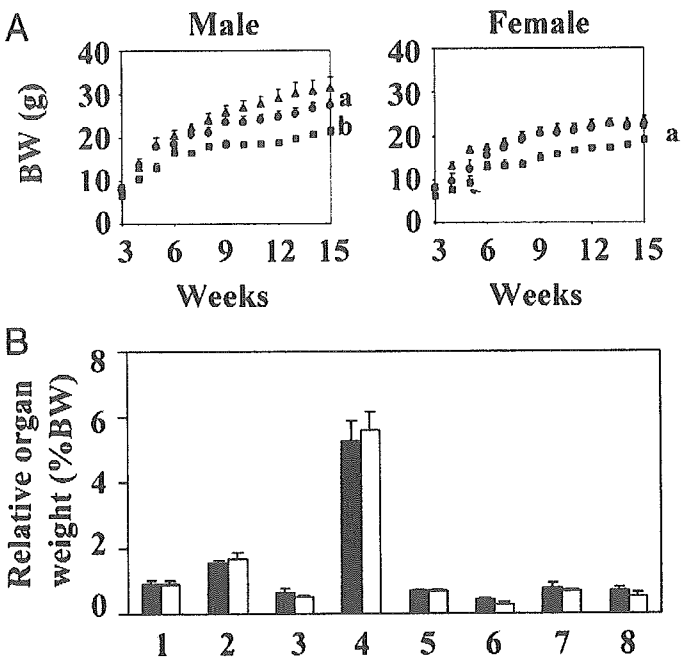

FIG. 2. Body weights (BW) and relative organ weights. A, Body weights of male (*left panel*) and female (*right panel*) control (*triangles*), Tg 9–2 (*circles*), and Tg 10–1 (*squares*) mice (n = 8/group). B, Relative organ weights of 8-wk-old control (*closed bars*) and Tg 10–1 (*open bars*) mice calculated from the organ and body weights (n = 8/group). 1, stomach; 2, cerebrum; 3, heart; 4, liver; 5, kidney; 6, spleen; 7, pancreas; 8, epididymal fat. a, $P < 0.05$; b, $P < 0.01$ (*vs.* control mice).

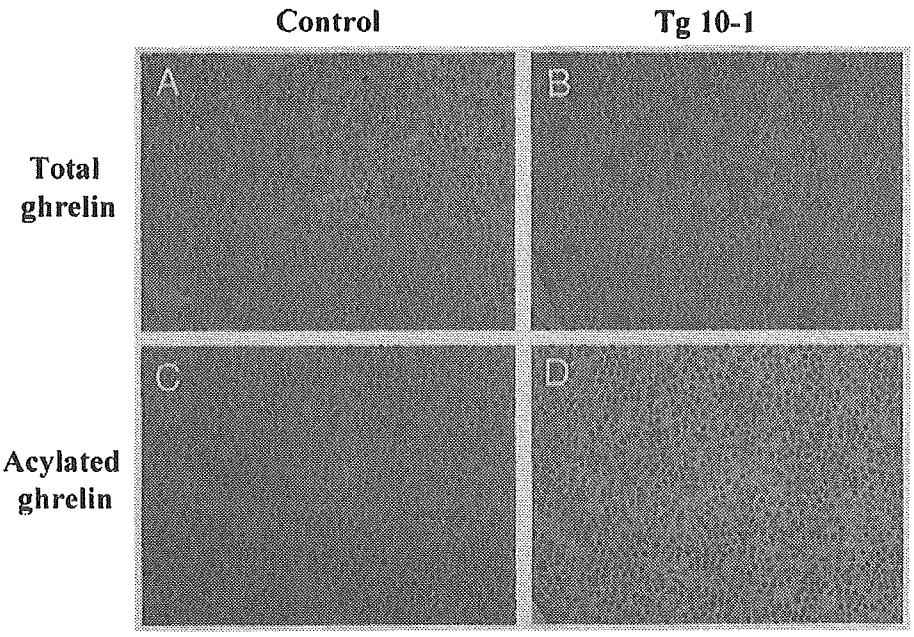

FIG. 3. The localization of total and acylated ghrelin-immunoreactive cells in the pituitary of 8-wk-old male control (A and C) and Tg 10–1 (B and D) mice. A and B, An antiserum raised to ghrelin(13–28) recognizing total (acylated plus des-acyl) ghrelin was used. C and D, An antiserum raised to ghrelin(1–11) specifically recognizing acylated ghrelin was used. Original magnification, ×40. The immunoreactive cells are stained *brown* by the avidin-biotin complex methods.

Food intake and biochemical parameters in the blood

Although absolute amounts of daily food intake were reduced in Tg 9–2 and Tg 10–1 mice, the amounts per body weight were not significantly changed in either male or female Tg 9–2 or Tg 10–1 mice, compared with control mice (Table 4). No significant differences in blood glucose, serum total protein, total cholesterol, and insulin levels were noted between 8-wk-old control and Tg 9–2 mice and control and Tg 10–1 mice (Table 4).

Serum GH, IGF-1, and pituitary GH mRNA levels

Serum GH levels in male control, Tg 9–2, and Tg 10–1 mice were 5.5 ± 1.9, 3.7 ± 0.7, and 2.3 ± 0.9 ng/ml, respectively (Fig. 4A). Those in female control, Tg 9–2, and Tg 10–1 mice were 4.7 ± 1.7, 2.5 ± 0.9, and 1.7 ± 0.8 ng/ml, respectively (Fig. 4A). There were tendencies for decline in serum GH levels in male and female Tg 9–2 and Tg 10–1 mice, compared with control mice, although the differences between them were not significant. Serum IGF-I levels in male control, Tg 9–2, and Tg 10–1 mice were 522 ± 23.6, 413.2 ± 49.0, and 364.1 ± 25.6 ng/ml, respectively (Fig. 4B). Those in male Tg 9–2 and Tg 10–1 mice were significantly reduced, compared with those in control mice ($P < 0.01$ for each). Serum IGF-I levels in female control, Tg 9–2, and Tg 10–1 mice were 509.7 ± 43.1, 545.5 ± 64.1, and 253.7 ± 36.4 ng/ml, respectively (Fig. 4B). Those in female Tg 10–1 mice were significantly reduced, compared with those in control mice ($P < 0.01$). The difference between female control and Tg 9–2 mice was not significant.

Pituitary GH mRNA levels in male control, Tg 9–2, and Tg 10–1 mice were 1.00, 0.62, and 0.42 AU, respectively. Those in Tg 9–2 and Tg 10–1 mice were significantly reduced, compared with those in control mice ($P < 0.05$ and $P < 0.01$, respectively). Pituitary GH mRNA levels in female control, Tg 9–2, and Tg 10–1 mice were 1.00, 0.97, and 0.71 AU. Those in female Tg 10–1 mice were significantly reduced, compared with those in control mice ($P < 0.05$). The difference between those in female control and Tg 9–2 mice was not significant (Fig. 4C).

Plasma ACTH, serum TSH, LH, and FSH levels

Plasma ACTH, serum TSH, LH, and FSH levels in 8-wk-old in male control and transgenic mice are shown in Table

TABLE 4. Daily food intake, blood glucose, serum total protein, total cholesterol, and insulin levels in 8-wk-old control and transgenic mice (n = 8/group)

	Control	Tg 9-2	Tg 10-1
Male			
Daily food intake (mg/BW/d)	149.1 ± 7.6	154.2 ± 3.2	155.2 ± 5.9
Serum total protein (mg/dl)	5.1 ± 0.2	4.9 ± 0.1	5.5 ± 0.1
Serum total cholesterol (mg/dl)	121.0 ± 12	116.9 ± 11.3	123.1 ± 8.3
Blood sugar (mg/dl)	134.2 ± 9.4	135.3 ± 8.7	136.7 ± 5.8
Serum insulin (pg/ml)	3233 ± 407	4624 ± 1015	2419 ± 423
Female			
Daily food intake (mg/BW/d)	167.5 ± 2.3	169.5 ± 4.7	165.8 ± 9.8
Serum total protein (mg/dl)	5.4 ± 0.1	5.1 ± 0.3	5.2 ± 0.3
Serum total cholesterol (mg/dl)	129.0 ± 9.3	123.4 ± 9.2	122.9 ± 6.1
Blood sugar (mg/dl)	132.1 ± 5.5	134.2 ± 6.4	130.6 ± 7.2
Serum insulin (pg/ml)	1182 ± 284	2079 ± 587	1799 ± 725

Values are given as the mean ± SEM. BW, Body weight.